

UNCLASSIFIED



AD 728502

MEMORANDUM 37

PREDICTION OF BALLISTIC MISSILE TRAJECTORIES

D D C
RECEIVED
AUG 20 1971
B

Distribution:

Gardiner	Ross
Dressler	Salmon
Meier	Eikelman
Ito	Fraser
Kashiwagi	Yabroff
Keckler	Albritton
Korsak	Belote
Lombard	Roscher
Luenberger	Moore
Hatner	Weinstein
	Branch

Davidson, NXPO
 Montgomery, NXPO
 Smyth, NXPO
 Wells, NXPO
 Young, NXPO

Reproduced by
**NATIONAL TECHNICAL
 INFORMATION SERVICE**
 Springfield, Va. 22151

Prepared by:
 Yasutada Kashiwagi
 June 1968
 Project 5188-305

SRI-H-8-976
 R3

UNCLASSIFIED

53

CONTENTS

LIST OF ILLUSTRATIONS	iii
LIST OF TABLES	iv
I INTRODUCTION	1
II EQUATION OF MOTION	2
III ENDOATMOSPHERIC PREDICTION	6
A. Characteristics of the Ballistic Trajectories in Endoatmosphere.	7
B. Influence of β in Endoatmosphere	11
C. Effect of Nonlinearity in Endoatmosphere	18
D. Influence of ω in Endoatmosphere	19
E. Effect of Eccentricity in Endoatmosphere	23
F. Approximation of Nonlinear Term in Endoatmosphere.	23
IV EXOATMOSPHERIC PREDICTION.	27
A. Effect of Nonlinearity in Exoatmosphere.	31
B. Approximation of Nonlinear Term in Exoatmosphere	32
C. Influence of ω in Exoatmosphere.	33
D. Influence of Eccentricity in Exoatmosphere	33
V SENSITIVITY OF IMPACT POINTS TO INITIAL VALUES	35
VI CONCLUSION	41
APPENDIX	42
REFERENCES.	49

ILLUSTRATIONS

Fig. 1 Coordinate System	2
Fig. 2 Density of the Atmosphere	8
Fig. 3 Ballistic Trajectories on the $x-y$ Plane, Case 1	9
Fig. 4 Ballistic Trajectories on the $z-x$ Plane, Case 1	10
Fig. 5 Ballistic Coefficient - Altitude Graph for $\beta_0, \beta_1, \beta_2$	12
Fig. 6 Ballistic Coefficient - Altitude Graph for $\beta_3, \beta_4, \beta_5$	13
Fig. 7 Ballistic Trajectories on the $x-y$ Plane, Case 2	14
Fig. 8 Ballistic Trajectories on the $z-x$ Plane, Case 2	15
Fig. 9 Ballistic Trajectories on the $x-y$ Plane, Case 3	16
Fig. 10 Ballistic Trajectories on the $z-x$ Plane, Case 3	17
Fig. 11 Influences of $e, \omega,$ and \underline{C} (Endoatmosphere, $\beta = \beta_0$), $x-y$ Plane.	20
Fig. 12 Influences of $e, \omega,$ and \underline{C} (Endoatmosphere, $\beta = \beta_0$), $z-x$ Plane.	21
Fig. 13 Influences of $e, \omega,$ and \underline{C} (Exoatmosphere), $x-y$ Plane.	28
Fig. 14 Influences of $e, \omega,$ and \underline{C} (Exoatmosphere), $z-x$ Plane.	29
Fig. A-1 Illustrations of Unit Vectors	46

TABLES

Table I	Influences of ϵ , ω , and \underline{C} (Endoatmosphere $\beta = \beta_0$)	22
Table II	Influences of ϵ , ω , and \underline{C} (Endoatmosphere $\beta = \beta_4$)	22
Table III	Approximations of Nonlinear Terms (Endoatmosphere, High $\beta = \beta_0$) $\dot{X} = \underline{AX} + \underline{B}$	24
Table IV	Approximations of Nonlinear Terms (Endoatmosphere Low $\beta = \beta_4$) $\dot{X} = \underline{AX} + \underline{B} + \underline{C}$	25
Table V	Influences of ϵ , ω , and \underline{C} (Exoatmosphere)	30
Table VI	Sensitivity of Impact Points to Initial Values (Endoatmosphere), 10% Error.	37
Table VII	Sensitivity of Impact Points to Initial Values (Endoatmosphere), 20% Error.	38
Table VIII	Sensitivity of Impact Points to Initial Values (Exoatmosphere), 10% Error.	39
Table IX	Sensitivity of Impact Points to Initial Values (Exoatmosphere), 20% Error.	40
Table X	Summary of Influences of ϵ , ω , \underline{C} , and β	41

I INTRODUCTION

A critical problem in a missile defense system is that of predicting the trajectory and impact point for a ballistic reentry vehicle. This memorandum will describe methods of prediction as well as numerical results for several representative examples. There are several reports^{1,2*} describing the estimation of the states of a ballistic missile; the ballistic trajectory and impact point will be predicted by using these estimated values.

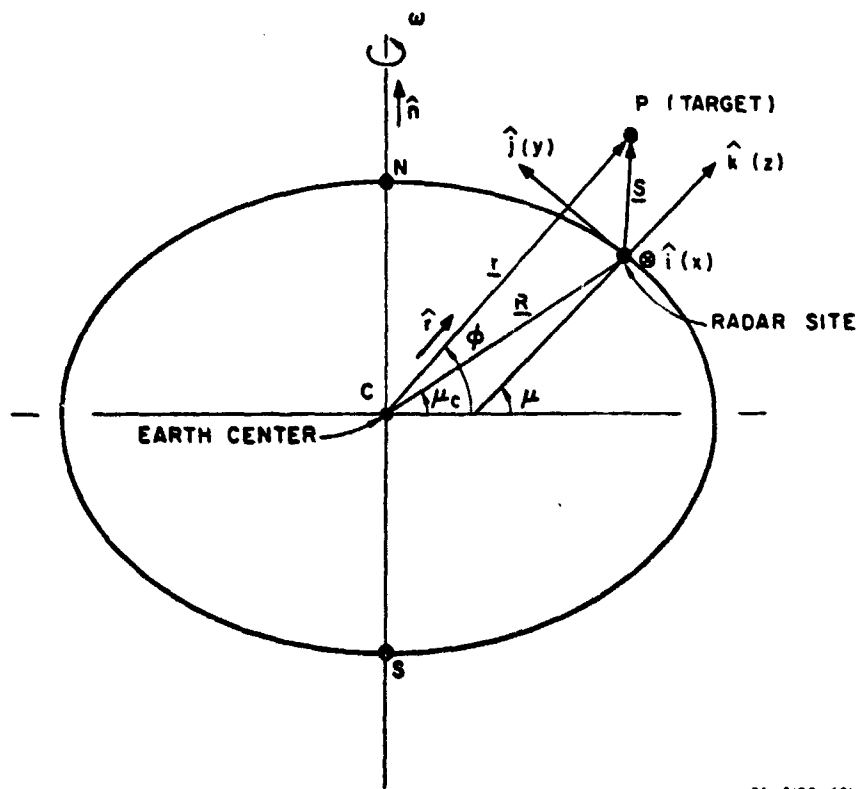
There are several important points to be considered. First is the choice of the coordinate system to be employed. Either a radar coordinate system or a rectangular coordinate system centered at the radar site can be used for the problems being studied. Second is the treatment of physical parameters in the equation of motion, such as the ballistic coefficient of the reentry vehicle and the eccentricity and rotation of the earth. Since the time required for computation may become significantly large, it is also very desirable to find a closed-form solution of the equation of motion, which is a rather complex nonlinear differential equation. The important point here is how much the accuracy of the solution is degraded in obtaining a closed-form solution. Third is the propagation of initial errors to the final values in prediction; this is valuable in order to trade off the magnitude of errors and the computation time in estimation. For this purpose, the sensitivity of the initial values to impact points is briefly investigated.

* References are listed at the end of the text.

II EQUATION OF MOTION

The following differential equation in state-variable form describes the motion of a ballistic missile; the derivation of this equation is shown in the Appendix and the coordinate system is shown in Fig. 1.

$$\dot{\underline{X}} = \underline{A}\underline{X} + \underline{B} + \underline{C} + \underline{D} \quad (1)$$



TA - 5100 - 401

FIG. 1 COORDINATE SYSTEM

where

$$\underline{A} = \begin{bmatrix} 0 & 0 & 0 & 1 & 0 & 0 \\ 0 & 0 & 0 & 0 & 1 & 0 \\ 0 & 0 & 0 & 0 & 0 & 1 \\ \omega^2 - \frac{GM}{r_0^3} & 0 & 0 & -\frac{\rho_B}{2\beta} V_0 & 2\omega \sin \mu & -2\omega \cos \mu \\ 0 & \omega^2 \sin^2 \mu - \frac{GM}{r_0^3} & -\omega^2 \sin \mu \cos \mu & -2\omega \sin \mu & -\frac{\rho_B}{2\beta} V_0 & 0 \\ 0 & -\omega^2 \sin \mu \cos \mu & \omega^2 \cos^2 \mu - \frac{GM}{r_0^3} & 2\omega \cos \mu & 0 & -\frac{\rho_B}{2\beta} V_0 \end{bmatrix}$$

$$\underline{B} = \begin{bmatrix} 0 \\ 0 \\ 0 \\ 0 \\ -\omega^2 R \sin \mu \cos \mu \\ \omega^2 R \cos^2 \mu - \frac{GM R}{r_0^3} \end{bmatrix}$$

$$\underline{C} = \begin{bmatrix} 0 \\ 0 \\ 0 \\ \frac{\rho_B}{2\beta} [V_0 - V] \dot{x} + GM \left(\frac{1}{r_0^3} - \frac{1}{r^3} \right) x \\ \frac{\rho_B}{2\beta} [V_0 - V] \dot{y} + GM \left(\frac{1}{r_0^3} - \frac{1}{r^3} \right) y \\ \frac{\rho_B}{2\beta} [V_0 - V] \dot{z} + GM \left(\frac{1}{r_0^3} - \frac{1}{r^3} \right) (z + R) \end{bmatrix}$$

$$\underline{D} = \begin{bmatrix}
 0 \\
 0 \\
 0 \\
 -\frac{GM}{r^3} J \left(\frac{a}{r}\right)^2 (1 - 5 \sin^2 \phi) x \\
 \hline
 -\frac{GM}{r^3} J \left(\frac{a}{r}\right)^2 (1 - 5 \sin^2 \phi) y - \frac{2GM}{r^2} J \left(\frac{a}{r}\right)^2 \sin \phi \cos \mu \\
 - R \omega^2 \sin \mu \{ \cos \mu [\cos(\mu - \mu_c) - 1] - \sin \mu \sin(\mu - \mu_c) \} \\
 + \frac{GM}{r^3} R \sin(\mu - \mu_c) \left[J \left(\frac{a}{r}\right)^2 (1 - 5 \sin^2 \phi) + 1 \right] \\
 \hline
 -\frac{GM}{r^3} J \left(\frac{a}{r}\right)^2 (1 - 5 \sin^2 \phi) [z + R \cos(\mu - \mu_c)] - \frac{2GM}{r^2} J \left(\frac{a}{r}\right)^2 \sin \phi \sin \mu \\
 + R \omega^2 \cos \mu \{ \cos \mu [\cos(\mu - \mu_c) - 1] + \sin \mu \sin(\mu - \mu_c) \} \\
 - \frac{GM}{r^3} R [\cos(\mu - \mu_c) - 1]
 \end{bmatrix}$$

in which

- \underline{X}^T = $[x, y, z, \dot{x}, \dot{y}, \dot{z}]$ = target state
- ω = Earth rotation rate
- GM = Product of gravitational constant and mass of earth
- μ = Geodetic latitude of radar
- μ_c = Geocentric latitude of radar
- ρ = Atmospheric mass density at target position
- β = Ballistic coefficient (i.e., weight-to-drag ratio)
- R = Earth radius to radar site
- r = Magnitude of position vector from earth center to target
- V = Velocity magnitude of target
- g = Gravitational acceleration
- r_0, V_0 and ρ_0 are the initial values of r, V and ρ

e = Eccentricity of reference ellipsoidal earth
($e^2 = 0.0066945$)

J = Dimensionless constant = 1.624×10^{-3}

ϕ = Geocentric latitude of target

a = Equatorial radius of earth (20,926,743 ft).

The linear coefficient matrix A is a 6×6 matrix whose elements are constant except for three elements containing the atmospheric mass density ρ . The vector B is constant and the vector C is a nonlinear term that will be negligible if V , the magnitude of the target velocity, and r , the magnitude of the position vector from the earth to the target, do not change significantly. The last term D contains the elements describing the influence of the eccentricity of the reference ellipsoidal earth. Hence, if eccentricity e is considered to be zero, then the term D vanishes.

One of the objectives of this report is to investigate simplifications of the differential equation described above. If the terms C and D are negligible, the differential equation will become $\dot{\underline{X}} = A\underline{X} + \underline{B}$. It is true that a linear differential equation with time varying coefficients is no better for finding an analytical solution than a nonlinear differential equation. However, if the time varying coefficients are approximated as constant for a certain time interval, then piecewise closed-form solutions can be obtained.

Based on physical considerations, it is helpful for the purpose of the following discussion to divide the atmosphere into two regions. One is called *exosphere*, defined as the space above an altitude of 300,000 ft; the other is called *endosphere*, defined as the space below an altitude of 300,000 ft.

III ENDOATMOSPHERIC PREDICTION

For ballistic missiles at an altitude of 300,000 ft with a range of 200 miles, it will take less than a minute for the high- β vehicles to impact and at most several minutes for the low- β vehicles. Therefore, the gravity gradient due to the oblateness of the earth is negligible, and the term \underline{D} can be omitted in the investigation of endoatmospheric trajectory prediction. The effect of the earth's rotation rate ω is also negligible, except for small deviations that are observed during the last 10,000 ft before impact. The impact point is defined in this report as the point at which a trajectory reaches an altitude of 10,000 ft.

Theoretical considerations and numerical results obtained indicate that the term \underline{C} in Eq. (1) is negligible for endoatmosphere prediction, and this is especially true for high- β missiles. An approximate differential equation describing the ballistic trajectory takes the form

$$\dot{\underline{X}} = \underline{AX} + \underline{B} \quad (2)$$

Moreover, if ω can be considered as zero, then the differential equation is simplified further and becomes

$$\dot{\underline{X}} = \begin{bmatrix} 0 & 0 & 0 & 1 & 0 & 0 \\ 0 & 0 & 0 & 0 & 1 & 0 \\ 0 & 0 & 0 & 0 & 0 & 1 \\ 0 & \frac{g}{r_0^3} & 0 & -\frac{rg}{2\beta} v_0 & 0 & 0 \\ 0 & 0 & \frac{g}{r_0^3} & 0 & -\frac{rg}{2\beta} v_0 & 0 \\ 0 & 0 & 0 & 0 & 0 & -\frac{rg}{2\beta} v_0 \end{bmatrix} \underline{X} + \begin{bmatrix} 0 \\ 0 \\ 0 \\ 0 \\ 0 \\ \frac{GM}{r_0^2} \end{bmatrix} \quad (3)$$

The above equation generates predicted trajectories, which are very close to the actual trajectories down to 50,000-ft altitude from an altitude of 300,000 ft. Hence, if the intercept altitude is higher than 50,000 ft, the differential Eq. (3) is a good approximation to the equation of motion for both high- β and low- β missiles. For prediction of the trajectory down to 10,000-ft altitude, the above differential equation is still a good mathematical model for high- β missiles.

The density of the atmosphere changes in a complex manner; an exponential curve was used to approximate the density-altitude curve. As Fig. 2 shows, this curve does not match exactly with the U.S. Standard Atmosphere 1962³. However, for the prediction of an impact point, this exponential model is sufficiently accurate.

Several characteristics of Eq. (1) in endoatmosphere are discussed in the following sections, and the sensitivity of impact points to initial values is mentioned in Sec. V.

A. Characteristics of the Ballistic Trajectories in Endoatmosphere

As shown by the numerical results (see Fig. 3), projections of the trajectories on the x - y plane are almost straight lines. If the initial conditions are the same for trajectories with different constant values of β , then the x - y projections of their trajectories will lie on top of each other with the high- β missiles flying further than the low- β missiles. The impact points lie on a straight line in the x - y plane regardless of β values.

From Fig. 3 it can be seen that the projections of ballistic trajectories on the x - y plane do not differ very much for different values of β . However, the projections of ballistic trajectories on the z - x plane differ slightly for different values of β (see Fig. 4).

The sensitivity of the impact point prediction to the ballistic coefficient β is a function of the value of β ; for low β the sensitivity is large, and for high β the sensitivity becomes small. Therefore, it is rather important to detect whether a target missile has low β or high β . In the high- β case, it is possible to predict the impact point with high accuracy. Any inaccuracy can be made smaller by re-estimating the ballistic coefficient. The major effect of β on the trajectory occurs at an altitude of less than 150,000 ft. Since β comes into the differential

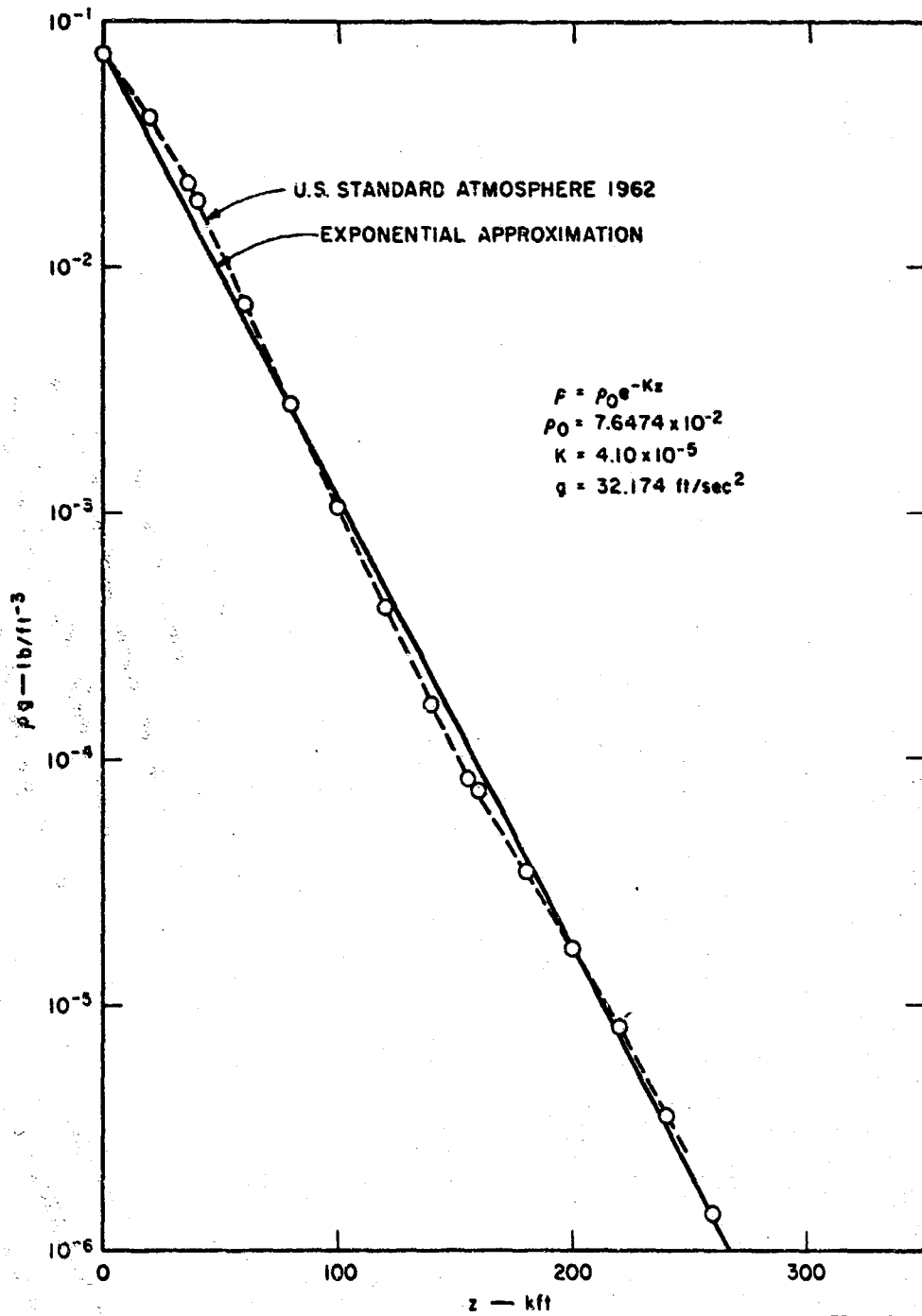


FIG. 2 DENSITY OF THE ATMOSPHERE

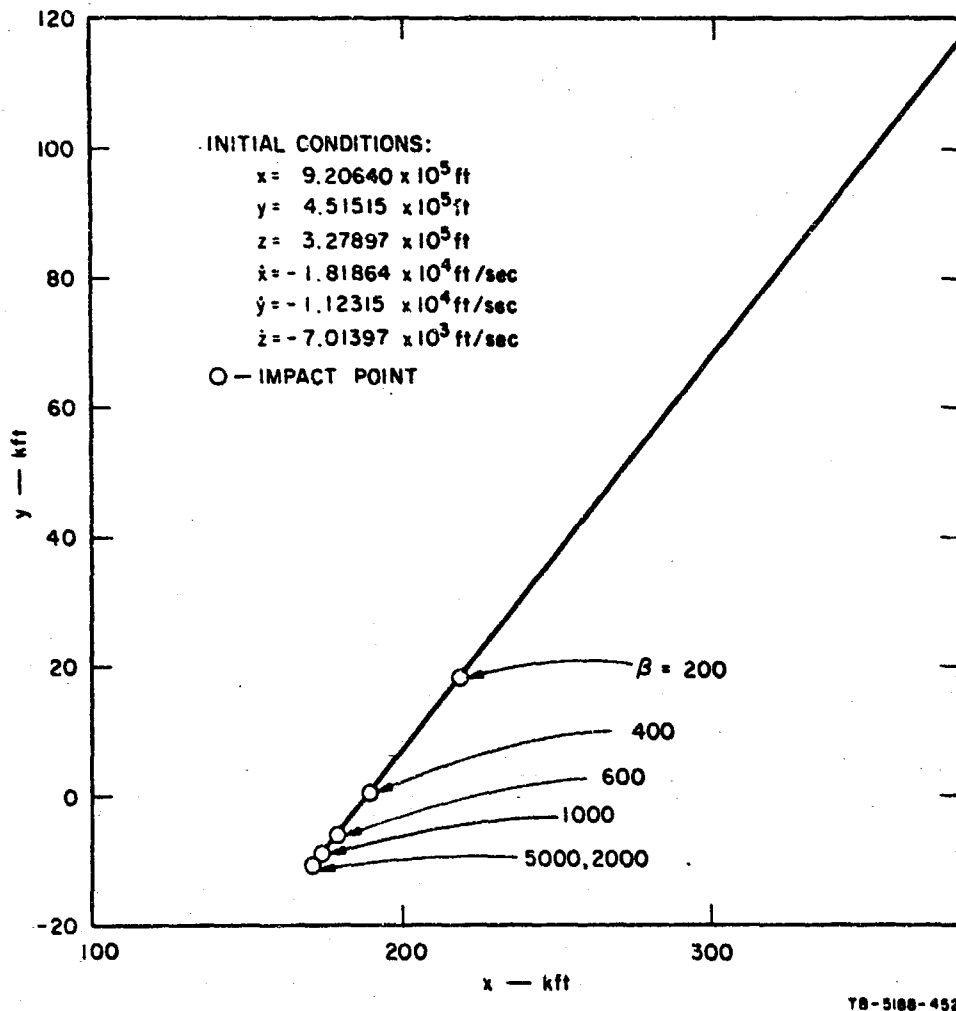


FIG. 3 BALLISTIC TRAJECTORIES ON THE x-y PLANE, CASE 1

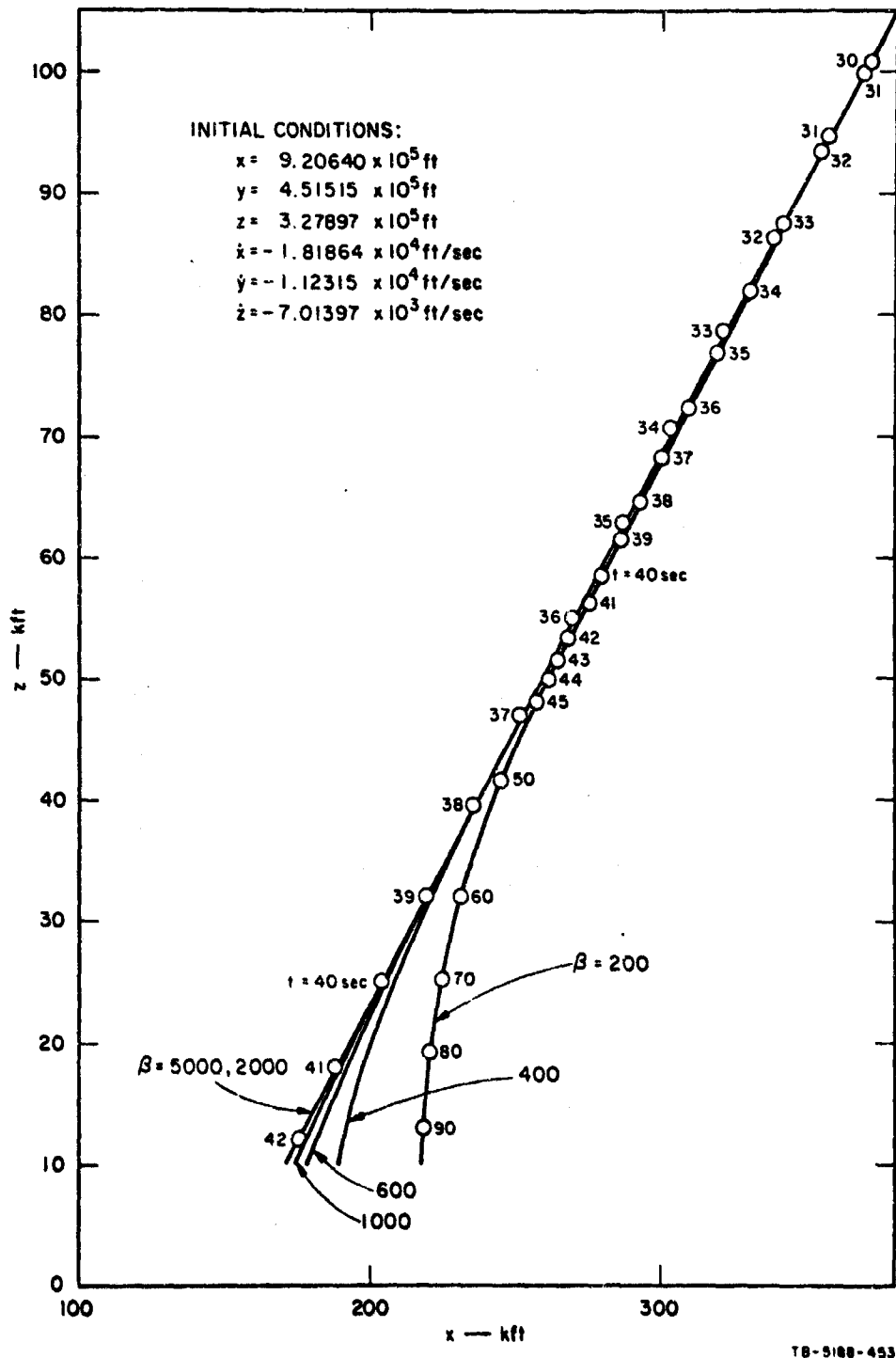


FIG. 4 BALLISTIC TRAJECTORIES ON THE z-x PLANE, CASE 1

equations in the form ρ/β and ρ is a very small value for high altitude, ρ/β is not a significant term unless the altitude is comparatively low (i.e., less than 150,000 ft).

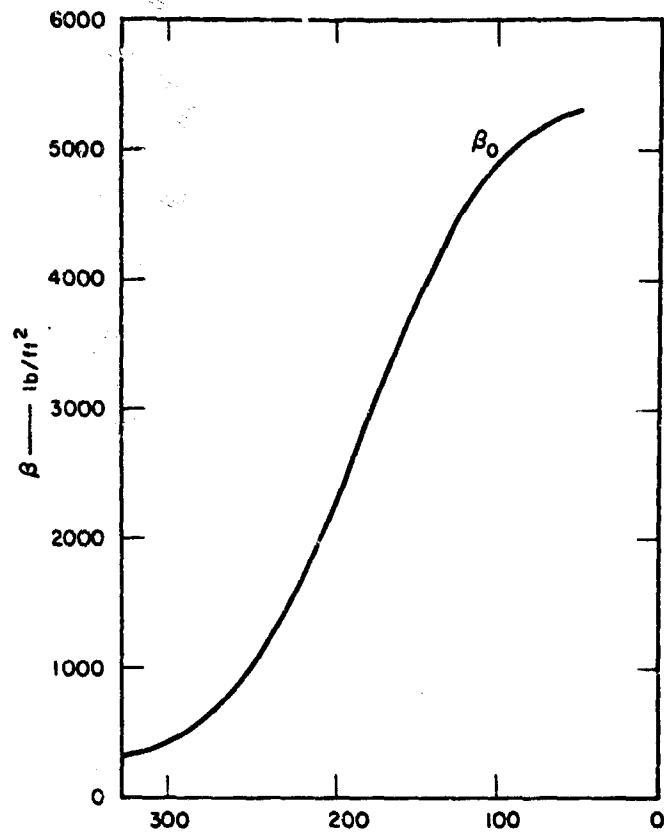
B. Influence of β in Endoatmosphere

In general, the shape of the β -altitude graph is parabolic-like and has a maximum value. Several examples are shown in Figs. 5 and 6. Experimental computations have been conducted by using the minimum, average, and maximum values for β . These results were then compared with the exact solution. The predicted trajectories and impact points for some representative cases are shown in Figs. 3, 4, 7, 8, 9, and 10. When the minimum value (constant) was used, the numerical results turned out to be quite different from the exact solution. On the other hand, if the maximum value (constant) of β is used, the deviation from the exact solution is not too large. For the case of high β , the maximum value will give the impact point without a significant error. However, the approximate value of β will cause an error in the impact time.

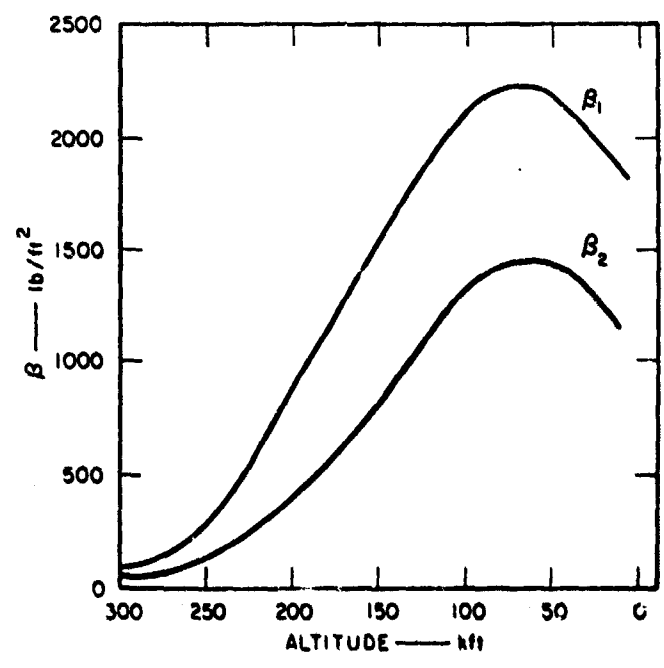
If a target missile is known to have a characteristic of high β , it is permissible to calculate the impact point by using a predicted maximum value of β or a value slightly smaller (by 10 to 20 percent) than the maximum value of β . If a target missile has a characteristic of low β , the prediction of the impact point will be more difficult than that for a high- β missile (refer to Figs. 3 and 4).

Consider the x-y projection of the trajectory. The impact points for high- β ballistic coefficients are very close to each other even though the β values are different. Some examples where β ranges from 1000 to 5000 lb/ft² show that the deviations are 5000 ft in the x direction and 3000 ft in the y direction at the impact point (refer to Figs. 3 and 4).

For low- β and high- β missiles having the same initial conditions and impacting on the surface of the earth, the impact points for the low- β missiles lie on the x-y projection of a trajectory for a high- β missile; in other words, the projections of low- β missiles on the x-y plane are shorter than those of high- β missiles. Moreover, the x-y projections of these trajectories are almost straight lines.



(a)



(b)

78-500-002

FIG. 5 BALLISTIC COEFFICIENT — ALTITUDE GRAPH FOR $\beta_0, \beta_1, \beta_2$

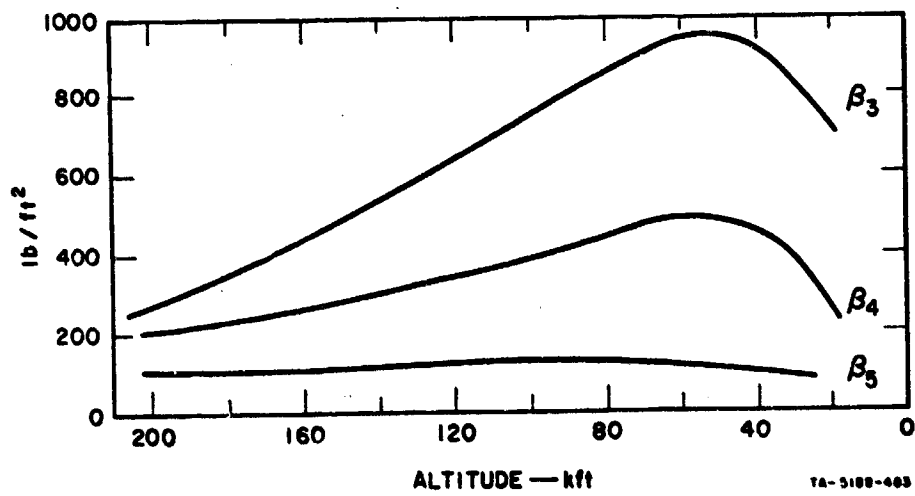
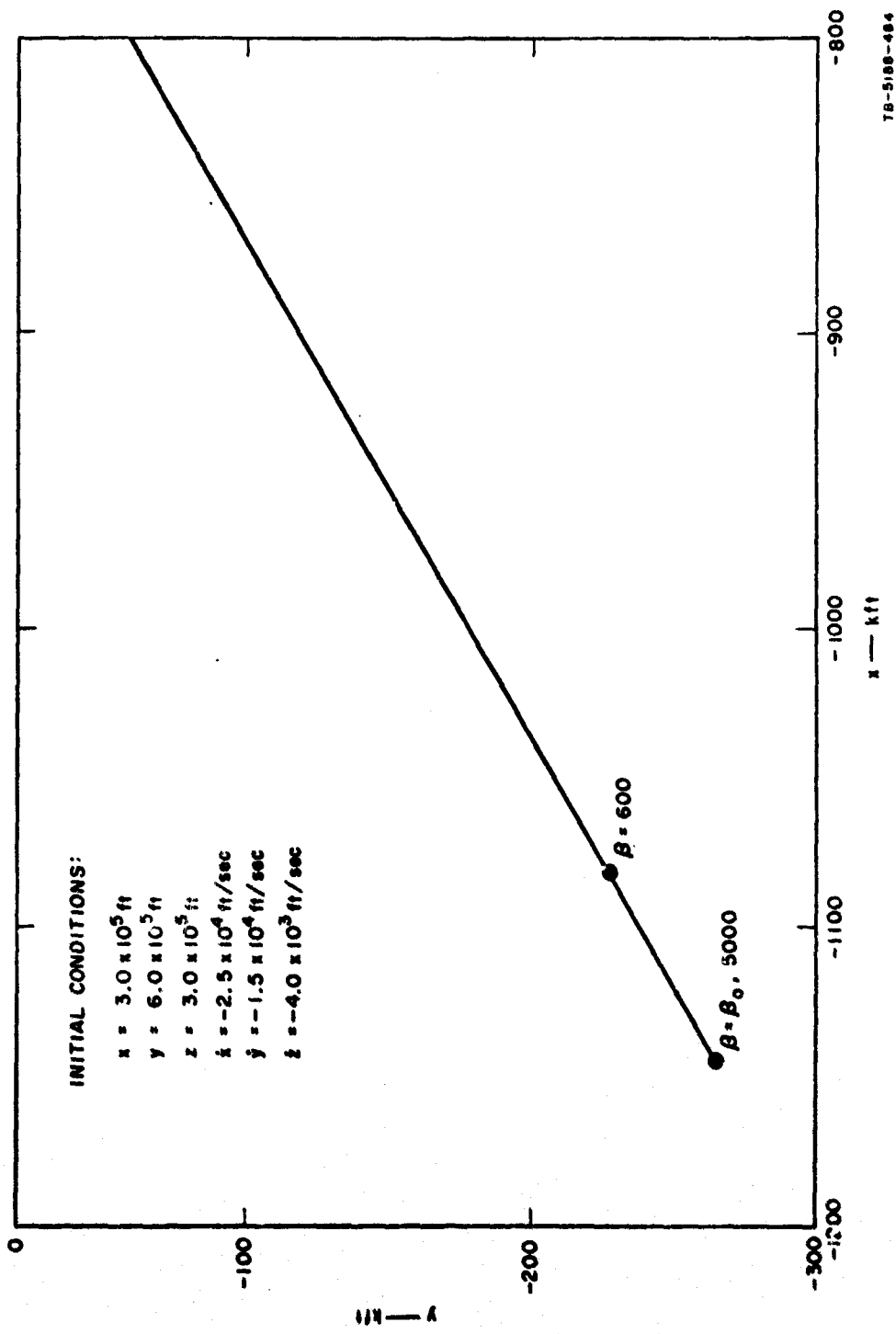
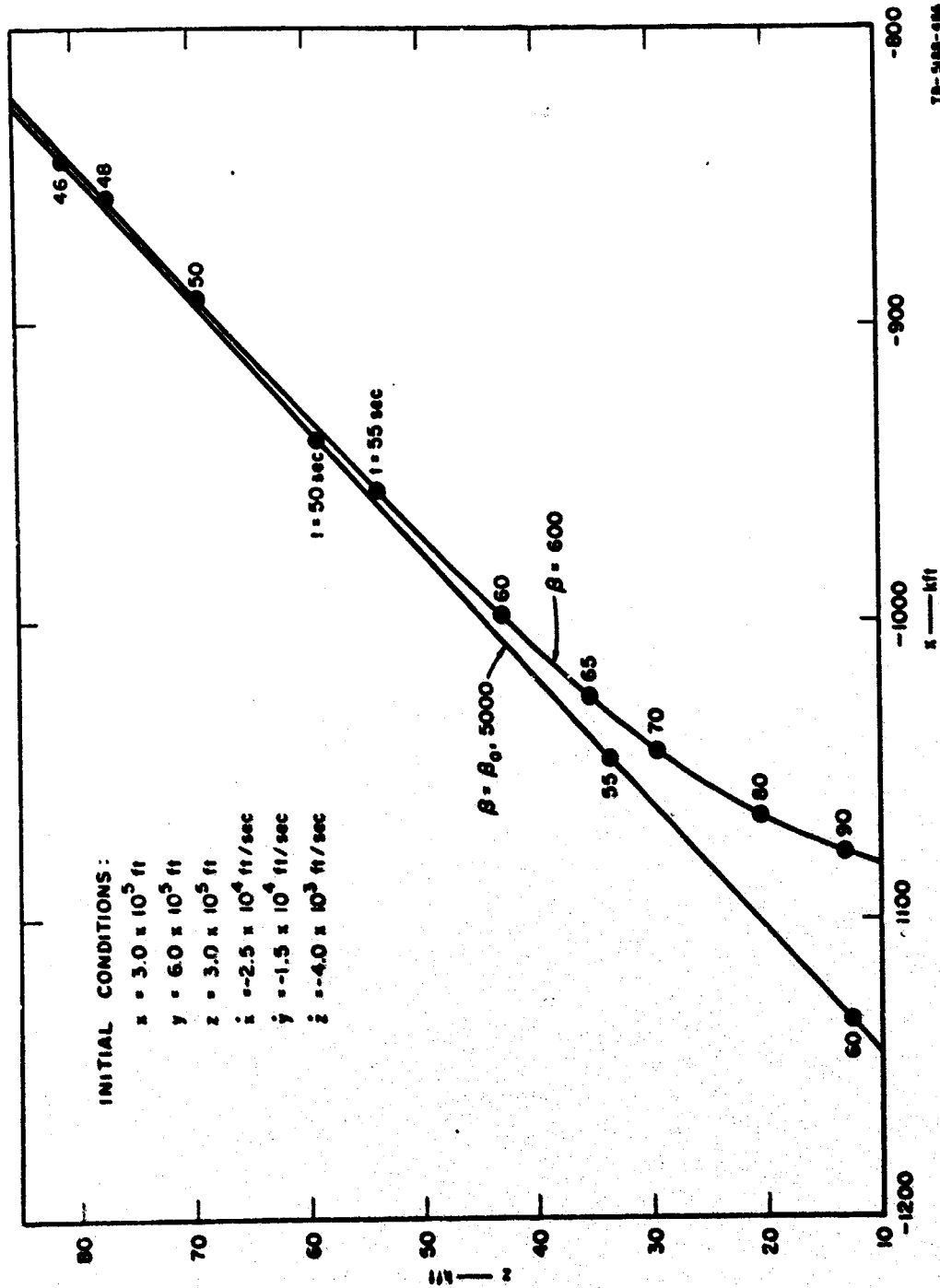


FIG. 6 BALLISTIC COEFFICIENT — ALTITUDE GRAPH FOR β_3 , β_4 , β_5



TR-5188-484

FIG. 7 BALLISTIC TRAJECTORIES ON THE x-y PLANE, CASE 2



78-588-486

FIG. 8 BALLISTIC TRAJECTORIES ON THE z-x PLANE, CASE 2

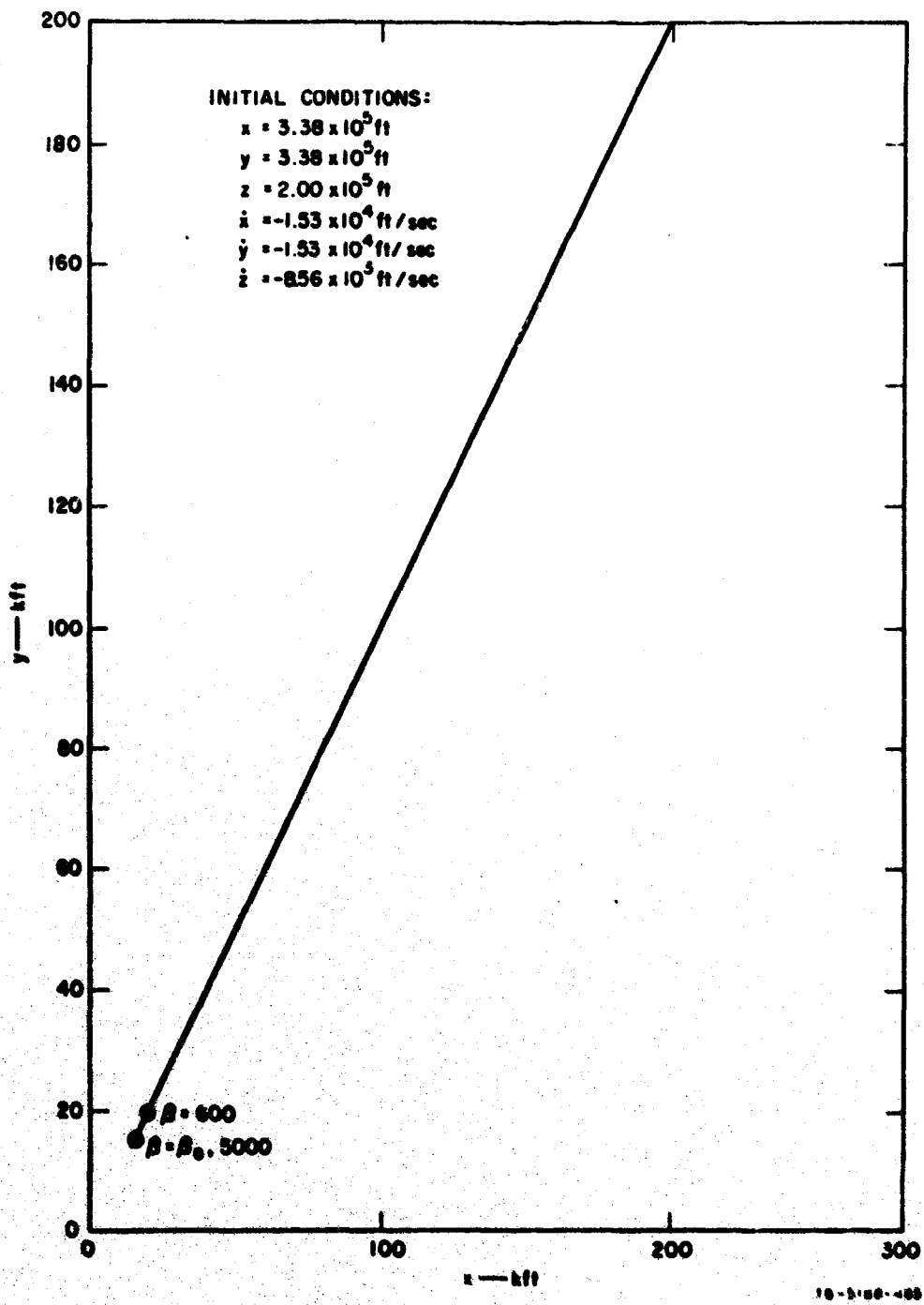


FIG. 9 BALLISTIC TRAJECTORIES ON THE x-y PLANE, CASE 3

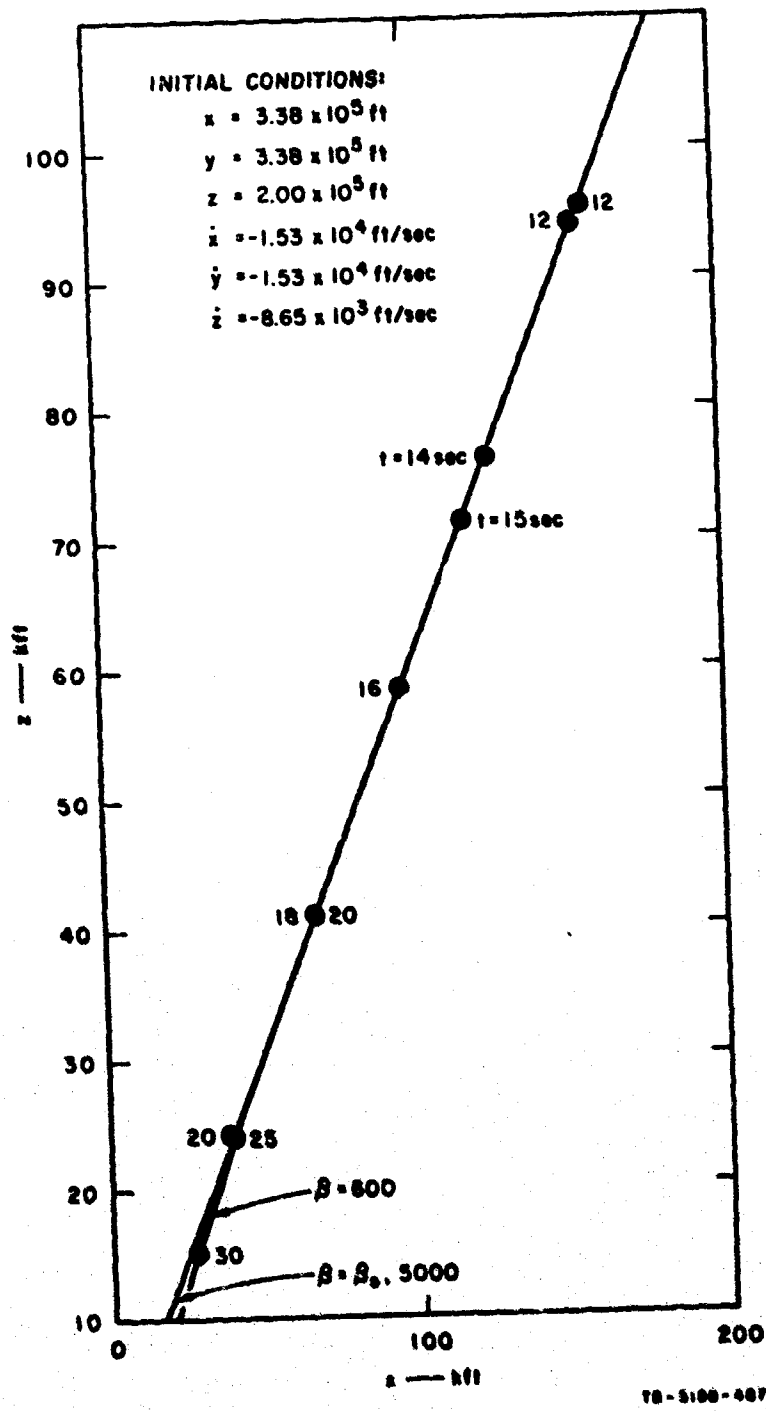


FIG. 10 BALLISTIC TRAJECTORIES ON THE z-x PLANE, CASE 3

Projections of trajectories on the $z-x$ plane for different values of β are again almost the same down to an altitude of 100,000 ft. Below 100,000 ft, the $z-x$ projections start separating and produce comparatively significant differences at impact. Some examples show that, because of different β values (from 200 to 5000 lb/ft²), projections of trajectories on the $x-y$ plane differ almost 50,000 ft in the x direction and 10,000 ft in the y direction (refer to Figs. 3, 4, 7, and 8).

Naturally the deviations differ according to the different values of the initial conditions. If the initial altitude is low and the descent speed \dot{z} is high, then the deviation due to the different values of β is not large. For comparison purposes one example of this kind is shown in Figs. 9 and 10.

C. Effect of Nonlinearity in Endoatmosphere

For endoatmospheric prediction, the nonlinear term \underline{C} is negligible if there is no significant change in values of r and V . In the endoatmosphere case the maximum deviation of r will be

$$\frac{r_0 - r(\text{impact})}{r(\text{impact})} \approx \frac{(a + 300,000) - a}{a} \approx 1.43 \times 10^{-5}$$

where a is the radius of the earth. Hence, the value $[1/r_0^3 - 1/r^3]$ in the term \underline{C} is negligible compared to $1/r_0^3$ for the endoatmospheric missile trajectories.

On the other hand, the value $[V_0 - V]$ in the term \underline{C} is not necessarily negligible compared to V_0 . Since a high- β missile does not slow down significantly, the value $[V_0 - V]$ is negligible compared to V_0 . The velocity of a low- β missile changes its velocity much more than that of a high- β missile. As a result, the value $[V_0 - V]$ is not negligible, and for some low- β missiles

$$\frac{V_0 - V}{V_0} \approx \frac{V}{V_0}$$

becomes 0.5 or greater.

In conclusion, for endoatmospheric prediction the term \underline{C} is negligible for high- β missiles, and the term \underline{C} should be handled carefully for low- β missiles. In order to illustrate the effects of the term \underline{C} on prediction, trajectories of high- β and low- β missiles are shown. Figures 11 and 12 and Table I show the high- β case, and Table II shows the low- β case.

D. Influence of ω in Endoatmosphere

For endoatmospheric prediction, the influence of the earth rotation rate ω is much more significant than that of the eccentricity e . An example of a high- β missile in the endoatmosphere is shown in Figs. 11 and 12 and Table I. With and without consideration of ω , the flight time difference is less than 0.5 sec and the deviation of the impact points is about 6400 ft (5000 ft in the x direction and 4000 ft in the y direction).

In this example, it takes about 43 sec to impact. A fixed point on the equator moves about 10 nautical miles during these 43 seconds. Then why is the deviation of the impact points with and without consideration of ω about 1 nautical mile rather than 10 nautical miles? The answer to this question is straightforward. The velocity of a target is measured with respect to the moving coordinate system, which is fixed to the earth at the radar site and rotates with the earth. Therefore, the deviation of impact points with and without ω is not caused by the motion of the radar site but is mainly caused by the effect of the coriolis term in Eq. (1).

Another example is shown in Table II. This is the case of a low- β missile in the endoatmosphere. The deviation of the impact points with and without consideration of ω is about 5000 ft (4000 ft in the x direction and 3000 ft in the y direction). Since this is a low- β missile, it takes about 74 sec to impact, which is about 80 percent longer than the time required for the high- β missile with the same initial conditions. The low- β missile takes a longer time to impact than the high- β missile, yet the deviation of impact points for the low- β missile with and without consideration of ω is smaller than that for the high- β missile. This is because the main contribution of ω is the coriolis term, which is proportional to the vector product $\underline{\omega} \times \underline{V}$ of the earth rotation rate and the velocity of the missile. Since $\underline{\omega}$ is constant, the effect due to coriolis term depends on the magnitude of \underline{V} . The higher the velocity of a missile, the larger the deviation that will occur.

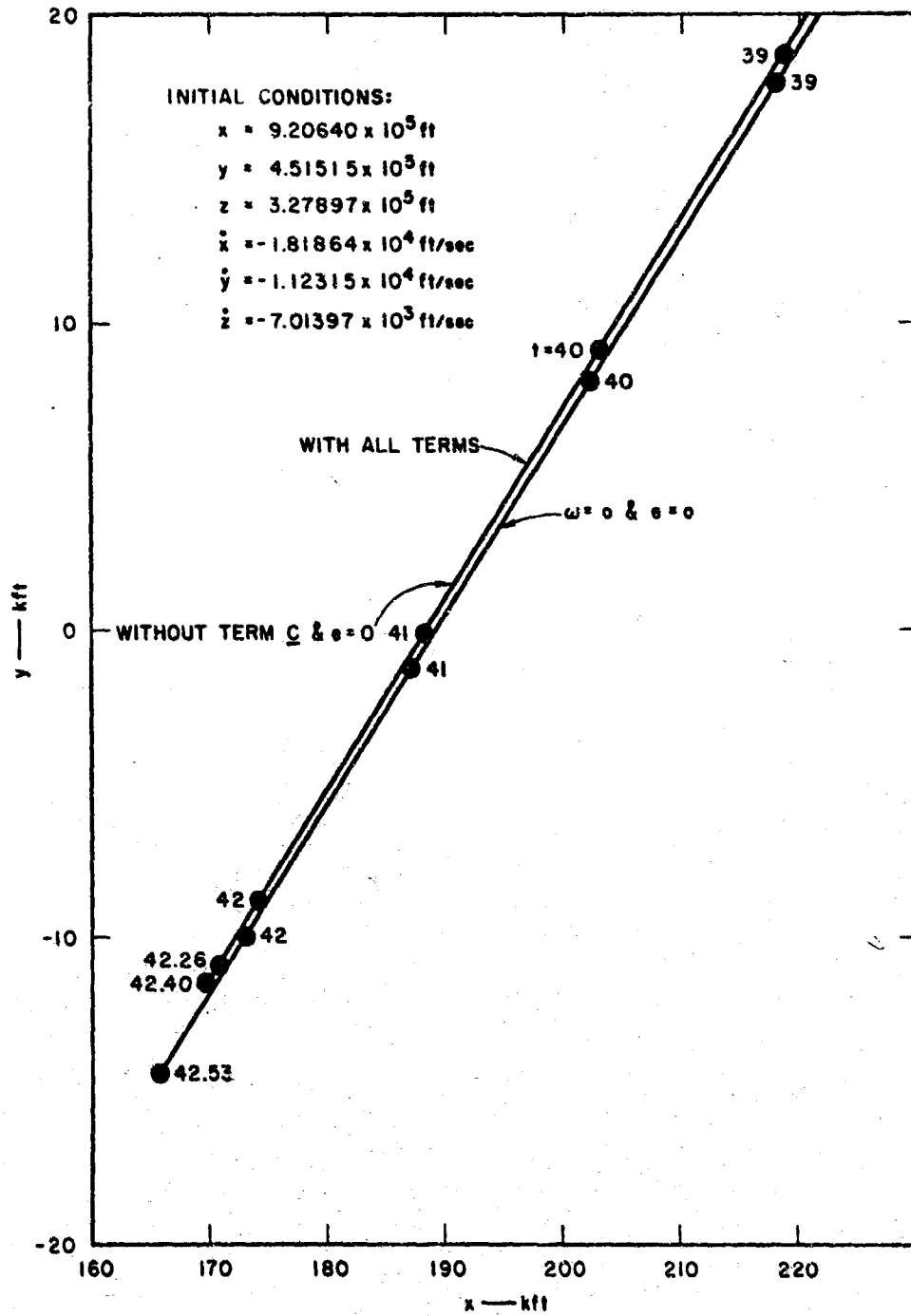


FIG. 11 INFLUENCES OF e , ω , AND c (Endoatmosphere, $\beta = \beta_0$), x-y PLANE

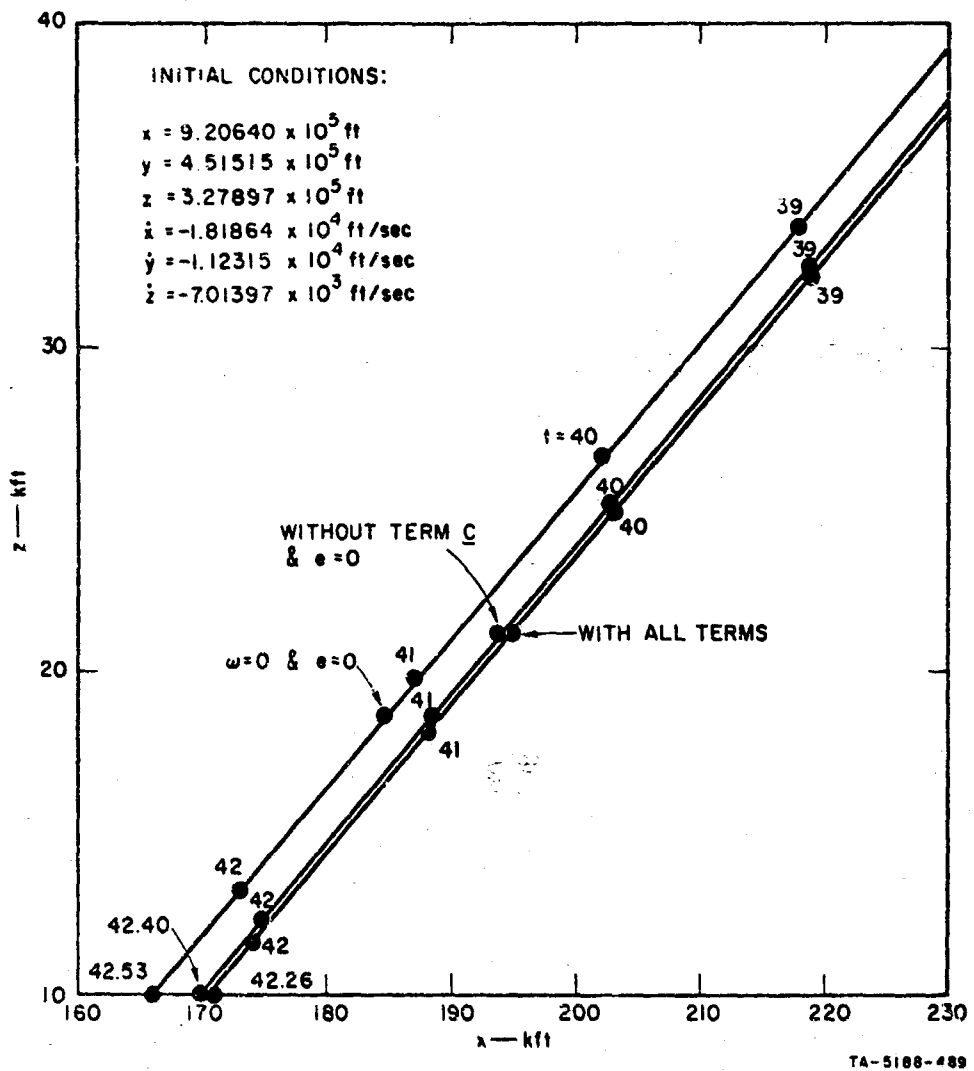


FIG. 12 INFLUENCES OF e , ω , AND \underline{C} (Endoatmosphere $\beta = \beta_0$), z-x PLANE

Table I
 INFLUENCES OF e , ω , and \underline{C} (ENDOATMOSPHERE $\beta = \beta_0$)

	x (ft)	y (ft)	z (ft)	\dot{x} (ft/sec)	\dot{y} (ft/sec)	\dot{z} (ft/sec)	\ddot{x} (ft/sec ²)	\ddot{y} (ft/sec ²)	\ddot{z} (ft/sec ²)	AT 10K FT: IMPACT TIME (sec)
Initial Conditions	9.20640×10^5	4.51515×10^5	3.27897×10^5	-1.81864×10^4	-1.12315×10^4	-7.01397×10^3				
With All Terms	1.70880×10^5	-1.08481×10^4	9.99887×10^3	-1.32036×10^4	-8.13048×10^3	-6.16264×10^3				42.26
$e = 0$	1.70706×10^5	-1.09852×10^4	9.99150×10^3	-1.32104×10^4	-8.13577×10^3	-6.16303×10^3				42.26
$e = 0, \omega = 0$	1.65871×10^5	-1.44627×10^4	9.99117×10^3	-1.31817×10^4	-8.13515×10^3	-6.07623×10^3				42.53
$e = 0$, Without term \underline{C}	1.69811×10^5	-1.15383×10^4	9.99217×10^3	-1.24773×10^4	-7.68427×10^3	-5.80415×10^3				42.40

Table II
 INFLUENCES OF e , ω , and \underline{C} (ENDOATMOSPHERE $\beta = \beta_1$)

	x (ft)	y (ft)	z (ft)	\dot{x} (ft/sec)	\dot{y} (ft/sec)	\dot{z} (ft/sec)	\ddot{x} (ft/sec ²)	\ddot{y} (ft/sec ²)	\ddot{z} (ft/sec ²)	AT 10K FT: IMPACT TIME (sec)
Initial Conditions	9.20640×10^5	4.51515×10^5	3.27897×10^5	-1.81864×10^4	-1.12315×10^4	-7.01397×10^3				
With All Terms	1.90872×10^5	1.45917×10^3	9.99558×10^3	-2.61121×10^2	-1.59612×10^2	-5.00749×10^2				73.92
$e = 0$	1.90778×10^5	1.43760×10^3	9.99929×10^3	-2.61100×10^2	-1.59183×10^2	-5.00344×10^2				73.95
$e = 0, \omega = 0$	1.86519×10^5	-1.66636×10^3	9.99364×10^3	-2.57739×10^2	-1.56926×10^2	-5.00760×10^3				74.70
$e = 0$, Without Term \underline{C}	2.42946×10^5	3.35366×10^4	3.96072×10^4	-9.30726×10^1	-2.39928×10^1	-8.05160×10				at 75.00

E. Effect of Eccentricity in Endoatmosphere

Eccentricity e comes into the differential equation of motion as the correction introduced into the gravitational force term due to the oblateness of the earth. The deviations of impact points with and without consideration of the eccentricity e are shown in Figs. 11 and 12 and in Tables I and II.

Figures 11 and 12 and Table I show the case of a high- β missile in endoatmosphere. The deviation is about 220 ft (180 ft in the x direction and 130 ft in the y direction). There is no difference in impact time.

Table II shows the case of a low- β missile in endoatmosphere. The deviation is about 100 ft (100 ft in the x direction and 22 ft in the y direction). The difference in impact time is about 0.03 sec.

In conclusion, the effect of the eccentricity e is entirely negligible for trajectory prediction in the endoatmosphere.

F. Approximation of Nonlinear Term in Endoatmosphere

As discussed in the previous sections, Eq. (1) can be approximated as

$$\dot{\underline{X}} = \underline{A}\underline{X} + \underline{B} \quad \text{for high } \beta \text{ missiles,} \quad (4)$$

and

$$\dot{\underline{X}} = \underline{A}\underline{X} + \underline{B} + \underline{C} \quad \text{for low } \beta \text{ missiles} \quad (5)$$

in endoatmospheric trajectory prediction.

If we consider ρ/β , r , and V to be piecewise constant, then the matrix \underline{A} and the term \underline{C} become piecewise constant. Hence, it is possible to find a piecewise closed-form solution for Eqs. (4) and (5). The accuracy of the solution depends upon the integration step size and the time interval during which ρ/β , r , and V are kept constant. Experimental computations were performed by taking five time intervals, namely, 1, 2, 3, 4, and 5 sec. The results are shown in Tables III and IV.

The purpose of obtaining a closed-form solution is to shorten the computation time to predict the missile trajectory. The approximation described above produces some inaccuracies. If the inaccuracies can be

Table III
 APPROXIMATIONS OF NONLINEAR TERMS (ENDOSPHERE, HIGH $\beta = \beta_0$), $\dot{X} = AX + \beta$

	\ddot{x} (ft)	\dot{x} (ft/sec)	x (ft)	\dot{x} (ft/sec)	\ddot{x} (ft/sec ²)	\dot{x} (ft/sec)	\ddot{x} (ft/sec ²)	AT 10K FT: IMPACT TIME (sec)
Initial Conditions	9.20640×10^5	4.51515×10^5	3.27897×10^5	-1.81864×10^4	-1.2315×10^5	-7.01397×10^3		
$\dot{X} = AX + B + C$ A, C: Variable	1.70706×10^5	-1.09852×10^4	9.99150×10^3	-1.32104×10^4	-8.13577×10^3	-6.16303×10^3	42.26	
$\dot{X} = AX + \beta$ A: Variable	1.70657×10^5	-1.10159×10^4	9.99944×10^3	-1.37471×10^4	-8.46635×10^3	-6.40511×10^3	42.12	
$\rho/\beta = \text{Constant}$ 1-sec correction	1.69751×10^5	-1.15758×10^4	9.99628×10^3	-1.31652×10^4	-8.10804×10^3	-6.11491×10^3	42.24	
$\rho/\beta = \text{Constant}$ 2-sec correction	1.69695×10^5	-1.16107×10^4	9.99793×10^3	-1.39136×10^4	-8.56907×10^3	-6.45405×10^3	42.10	
$\rho/\beta = \text{Constant}$ 3-sec correction	1.69630×10^5	-1.16509×10^4	9.99007×10^3	-1.45526×10^4	-8.96268×10^3	-6.74362×10^3	41.98	
$\rho/\beta = \text{Constant}$ 4-sec correction	1.69592×10^5	-1.16745×10^4	9.99098×10^3	-1.46899×10^4	-9.04728×10^3	-6.80210×10^3	41.89	
$\rho/\beta = \text{Constant}$ 5-sec correction	1.69557×10^5	-1.16962×10^4	9.99007×10^3	-1.49874×10^4	-9.23060×10^3	-6.93529×10^3	41.81	

Table IV
 APPROXIMATIONS OF NON-LINEAR TERMS (ENDOSPHERE, LOW $\beta = \beta_4$), $\dot{X} = AX + \underline{B} + \underline{C}$

	\dot{f}_0	\dot{f}_1	\dot{f}_2	\dot{f}_3	\dot{f}_4	\dot{f}_5	\dot{f}_6	\dot{f}_7	\dot{f}_8	AT 10K FT: IMPACT TIME (sec)
Initial Conditions	9.20646×10^5	4.51515×10^5	3.27897×10^5	-1.81864×10^4	-1.12315×10^5	-7.01397×10^3				
$\dot{X} = AX + \underline{B} + \underline{C}$ A, C: variable	1.90778×10^5	1.43760×10^3	9.99929×10^3	-2.61100×10^2	-1.59183×10^2	-5.00344×10^2				73.95
$\rho/\beta, r, V = \text{Const}$ 1-sec correction	1.88829×10^5	2.31232×10^3	9.99262×10^3	-2.73134×10^2	-1.66616×10^2	-4.97331×10^2				72.25
$\rho/\beta, r, V = \text{Const}$ 2-sec correction	1.86336×10^5	-1.31061×10^3	9.99434×10^3	-3.04590×10^2	-1.86041×10^2	-4.91385×10^2				69.69
$\rho/\beta, r, V = \text{Const}$ 3-sec correction	1.83835×10^5	-2.85721×10^3	9.99407×10^3	-3.47113×10^2	-2.12300×10^2	-4.85254×10^2				66.89
$\rho/\beta, r, V = \text{Const}$ 4-sec correction	1.81298×10^5	-4.42649×10^3	9.99184×10^3	-4.10032×10^2	-2.51142×10^2	-4.82257×10^2				63.72
$\rho/\beta, r, V = \text{Const}$ 5-sec correction	1.78916×10^5	-5.89958×10^3	9.99596×10^3	-5.15301×10^2	-3.16096×10^2	-4.90853×10^2				60.24

tolerated, a closed-form solution should be used in order to reduce the computation time.

As a reference, it may be helpful to give an approximate computation time to solve the differential Eq. (1) numerically. If the iteration step size Δt is taken as 100 msec and if one iteration does not exceed 0.2 msec, then the numerical calculation of a missile trajectory for a 50-sec flight requires less than 0.1 sec of computation time.

IV EXOATMOSPHERIC PREDICTION

In this report, the exoatmosphere is defined as the space above altitude 300,000 ft. Since the characteristics of the motion of ballistic missiles in the endoatmosphere and exoatmosphere are significantly different, it is very meaningful to obtain schemes of predicting trajectories separately.

As discussed in Sec. III, the equation of motion of missiles in endoatmosphere is described by Eqs. (2) or (3). The equation of motion of missiles in exoatmosphere can be approximated as

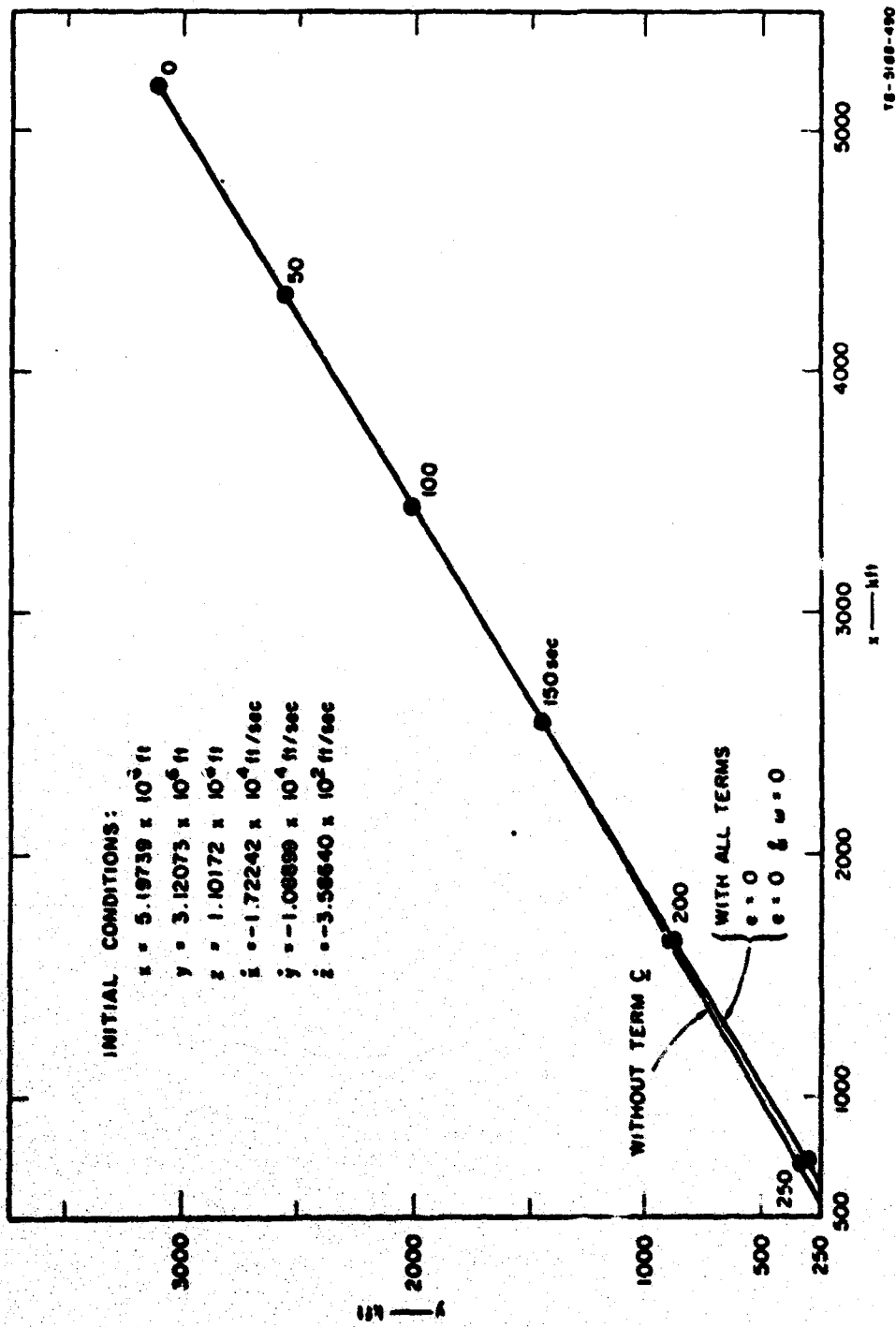
$$\dot{\underline{X}} = \underline{A}\underline{X} + \underline{B} + \underline{C} \quad (6)$$

Projections of the trajectories in exoatmosphere on the x-y plane are almost straight lines. Projections of trajectories on the z-x plane have the shape of an ellipse or a parabola. One example is shown in Figs. 13 and 14 and Table V.

The values of ρg is 1.488×10^{-7} lb ft⁻³ at altitude 300,000 ft ($\rho g = 7.6474 \times 10^{-2}$ lb ft⁻³ at the earth surface). Therefore, the element $(\rho g/2\beta)V$ has very little influence on the solutions regardless of the value of β . The classification of missiles is no longer meaningful in exoatmospheric prediction problems. If we consider the term $(\rho g/2\beta)V$ to be negligible, then Eq. (6) is simplified as

$$\dot{\underline{X}} = \tilde{\underline{A}}\underline{X} + \underline{B} + \underline{C} \quad (7)$$

where



78-5188-490

FIG. 13 INFLUENCES OF ϵ , ω , AND C (Exoatmosphere), x-y PLANE

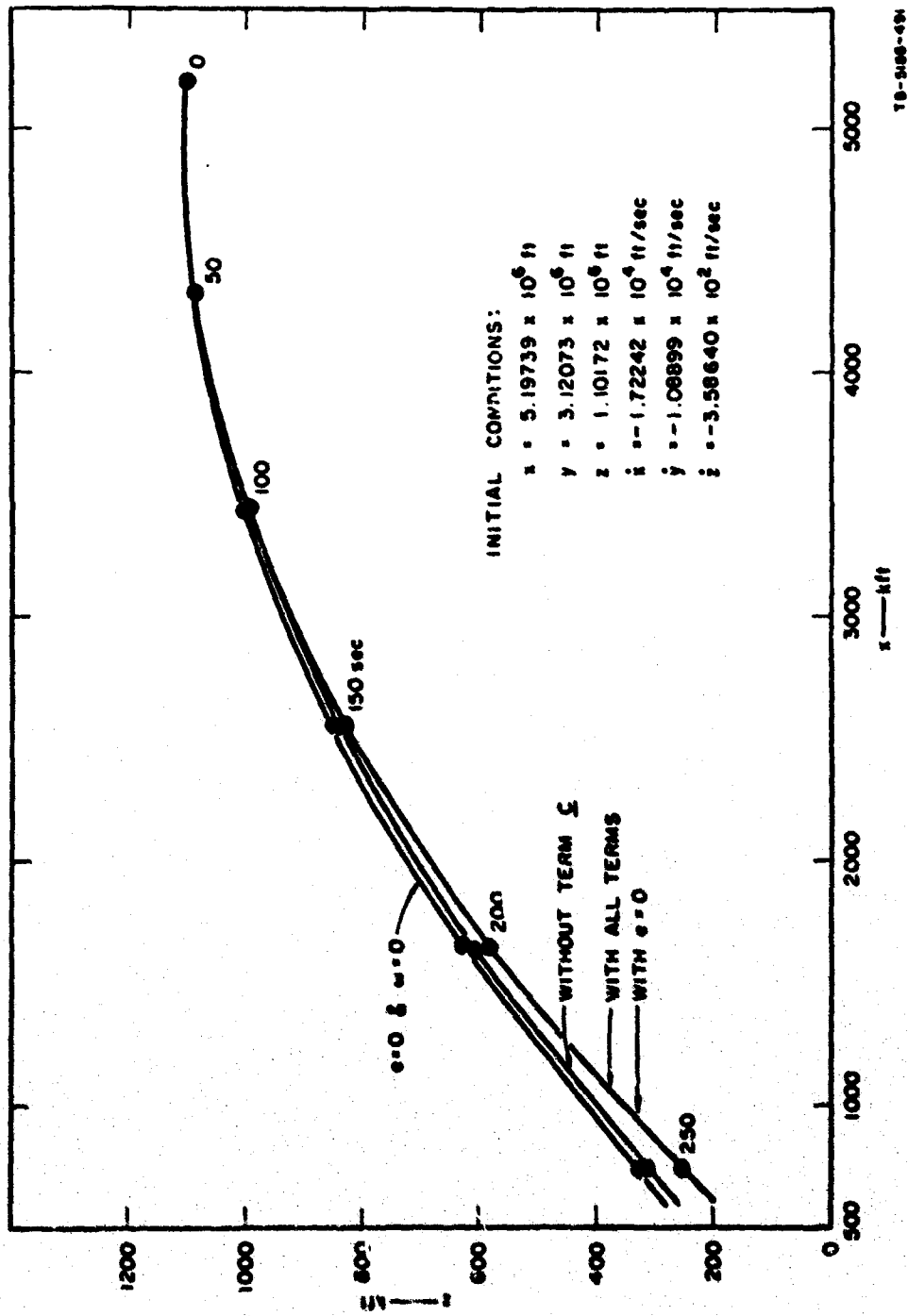


FIG. 14 INFLUENCES OF e , ω , AND ζ (Exatmosphere), z-x PLANE

Table V
 INFLUENCES OF ϵ , ω , AND ζ (EXOTATMOSPHERE)

	ϵ (ft)	γ (ft)	δ (ft)	ϵ^2 (ft ² /sec)	γ^2 (ft ² /sec)	δ^2 (ft ² /sec)	ϵ^3 (ft ³ /sec)	γ^3 (ft ³ /sec)	δ^3 (ft ³ /sec)	TIME (sec)
Initial conditions	5.19739×10^6	3.12073×10^6	1.10172×10^6	-1.72212×10^4	-1.72212×10^4	-1.72212×10^4	-1.08899×10^3	-1.08899×10^3	-1.08899×10^3	0
With all terms	9.20525×10^5	1.52091×10^5	3.26270×10^5	-1.81873×10^4	-1.81873×10^4	-1.81873×10^4	-1.12262×10^3	-1.12262×10^3	-1.12262×10^3	240
$\epsilon = 0$	9.20719×10^5	1.51528×10^5	3.28355×10^5	-1.81859×10^4	-1.81859×10^4	-1.81859×10^4	-1.12315×10^3	-1.12315×10^3	-1.12315×10^3	240
$\omega = 0$	9.28256×10^5	1.27508×10^5	3.94601×10^5	-1.81623×10^4	-1.81623×10^4	-1.81623×10^4	-1.14322×10^3	-1.14322×10^3	-1.14322×10^3	240
$\zeta = 0$, without ζ	9.26939×10^5	1.51327×10^5	3.76337×10^5	-1.81262×10^4	-1.81262×10^4	-1.81262×10^4	-1.11913×10^3	-1.11913×10^3	-1.11913×10^3	240
$\epsilon = 0$, with ζ	9.23019×10^5	1.52962×10^5	3.41456×10^5	-1.81684×10^4	-1.81684×10^4	-1.81684×10^4	-1.12204×10^3	-1.12204×10^3	-1.12204×10^3	240
10 sec correction										
$\epsilon = 0$, with ζ	9.21912×10^5	1.52253×10^5	3.36413×10^5	-1.81774×10^4	-1.81774×10^4	-1.81774×10^4	-1.12260×10^3	-1.12260×10^3	-1.12260×10^3	240
16 sec correction										
$\epsilon = 0$, with ζ	9.21235×10^5	1.51829×10^5	3.31523×10^5	-1.81625×10^4	-1.81625×10^4	-1.81625×10^4	-1.12293×10^3	-1.12293×10^3	-1.12293×10^3	240
10 sec correction										
With all terms	4.15264×10^6	2.46262×10^6	1.07166×10^6	-1.75899×10^4	-1.75899×10^4	-1.75899×10^4	-1.10109×10^3	-1.10109×10^3	-1.10109×10^3	60
$\epsilon = 0$	4.15265×10^6	2.46260×10^6	1.07179×10^6	-1.75893×10^4	-1.75893×10^4	-1.75893×10^4	-1.10319×10^3	-1.10319×10^3	-1.10319×10^3	60

$$\tilde{A} = \begin{bmatrix} 0 & 0 & 0 & 1 & 0 & 0 \\ 0 & 0 & 0 & 0 & 1 & 0 \\ 0 & 0 & 0 & 0 & 0 & 1 \\ \omega^2 - \frac{GM}{r_0^3} & 0 & 0 & 0 & 2\omega \sin \mu & -2\omega \cos \mu \\ 0 & \omega^2 \sin^2 \mu - \frac{GM}{r_0^3} & -\omega^2 \sin \mu \cos \mu & -2\omega \sin \mu & 0 & 0 \\ 0 & -\omega^2 \sin \mu \cos \mu & \omega^2 \cos^2 \mu - \frac{GM}{r_0^3} & 2\omega \cos \mu & 0 & 0 \end{bmatrix}$$

$$\underline{C} = \begin{bmatrix} 0 \\ 0 \\ 0 \\ GM \left(\frac{1}{r_0^3} - \frac{1}{r^3} \right) x \\ GM \left(\frac{1}{r_0^3} - \frac{1}{r^3} \right) y \\ GM \left(\frac{1}{r_0^3} - \frac{1}{r^3} \right) (z + R) \end{bmatrix}$$

In the following sections, we will discuss the degree of the accuracy of the above approximations in Eqs. (6) and (7).

A. Effect of Nonlinearity in Exoatmosphere

As discussed before, the nonlinear term \underline{C} is negligible for high- β missiles in endoatmosphere. However, the term \underline{C} should be handled carefully for low- β missiles in endoatmosphere.

The effect of nonlinear term \underline{C} (or \tilde{C}) is not negligible for any missile in exoatmosphere. This is due to the significant changes in the values of r and V during the flight. One example is shown in Figs. 13 and 14. If the flight time is reasonably small, then the changes in the values of r and V are negligible even in exoatmosphere. Hence, one way of handling the term \underline{C} (or \tilde{C}) is to make it piecewise constant. This

approximation allows us to reduce Eqs. (6) and (7) to linear differential equations with constant coefficients. As a result, it is possible to obtain a piecewise closed-form solution. This approach is discussed in the next section.

B. Approximation of Nonlinear Term in Exoatmosphere

In the Nike-Zeus system, prediction of the trajectory of a reentry vehicle is based on an analytical closed-form solution of an approximate set of equations of motion.⁴ In order to obtain an analytic solution to the equations, the effect of gravity is omitted, and the resulting predictions are corrected for gravity. This is one way of approximating the original differential equation to find a closed-form solution.

Another approach is to divide the total flight time into several intervals and to find a closed-form solution for each interval. In other words, term \underline{C} is eliminated and the initial values of r and V [only r in Eq. (7)] are used for a certain time interval $[0, \Delta t]$. The values of r and V are recalculated by using the state values at time Δt , and these revised constant values of r and V are used for calculating the trajectory for the next time interval $[\Delta t, 2\Delta t]$. This same procedure is continued until impact is reached.

This idea is demonstrated for an exoatmospheric trajectory, and the results are tabulated in Table V. The deviations of the predicted position from the exact value after 240-sec flight are the following:

50,000 ft	-----	without term \underline{C}
20,000 ft	-----	60-sec correction of r and V in \underline{C}
10,000 ft	-----	30-sec correction of r and V in \underline{C}
5,000 ft	-----	10-sec correction of r and V in \underline{C}

The more frequently corrections are made, the more accurately we will obtain solutions. The suitable number of intervals for dividing the total time depends on the error constraints.

If the total time T is divided into N intervals of Δt , then the original equation is approximated as

$$\dot{\underline{X}}_n(t) = A_n \underline{X}_n(t) + \underline{B}_n \quad \text{for} \quad n\Delta t \leq t \leq (n+1)\Delta t$$

$$n = 0, 1, \dots, \frac{T}{\Delta t}$$

and the initial conditions are defined as

$$\underline{X}_0(0) = \underline{X}_0$$

$$\underline{X}_n(n\Delta t) = \underline{X}_{n-1}[(n+1)\Delta t], \quad n = 1, 2, \dots, \frac{T}{\Delta t}$$

In the case of exoatmospheric trajectories, β is negligible; hence, A_n and B_n can be considered to be constant.

C. Influence of ω in Exoatmosphere

An example of a missile trajectory in exoatmosphere is shown in Figs. 13, 14, and Table V. The deviation of the impact points (compared at the same time rather than at the same altitude) with and without consideration of ω is about 75,000 ft (8,000 in the x direction, 25,000 ft in the y direction and 70,000 ft in the z direction) after 240 sec of flight.

The velocity of the missile in this example is much larger than that in endoatmosphere examples shown previously. Hence, the effect of the coriolis term is greater.

Although the effect of ω is negligible for endoatmospheric trajectory predictions, the effect is very significant for exoatmospheric trajectory predictions.

D. Influence of Eccentricity in Exoatmosphere

Figures 13, 14, and Table V show the case of a missile in exoatmosphere. The deviation of impact points with and without consideration of the eccentricity e is about 2100 ft (200 ft in the x direction, 500 ft in the y direction and 2000 ft in the z direction). The eccentricity e is negligible (with certain reservation) for the cases in exoatmosphere.

The main objective of neglecting the term D containing the eccentricity e is to simplify the differential equation in order to obtain a closed-form solution. For exoatmospheric trajectories, the deviation can be as large as 0.5 nautical miles after a 240-sec flight. If the tolerance of the error is several miles, then the eccentricity e can be considered as zero. If eccentricity e cannot be considered as zero, then it is clearly difficult to find a closed-form solution.

One way to overcome this difficulty is to find an efficient numerical integration technique. It is feasible to obtain a solution of the differential equation (1) by using about 0.5 sec of computer time on a present-day computer (e.g., UNIVAC 1108). The flight time for these exo-atmospheric cases is on the order of 5 minutes or more; therefore, 0.5 sec can be well justified for the computer calculations.

It is also possible to neglect the effect of eccentricity e and to simplify the differential equation so that the closed-form solution can be found. In order to support the above statement, it is useful to tabulate the state values at 60 sec after the initial time for trajectories with and without consideration of the eccentricity e . The last two rows of Table V show that the deviation is about 160 ft after 60 sec.

V SENSITIVITY OF IMPACT POINTS TO INITIAL VALUES

When the state values of an incoming missile are estimated, some errors are inevitable. In order to reduce errors, the computation time must be increased significantly. The knowledge of the propagation of initial errors to the final values in prediction is very meaningful in order to evaluate the trade-off between the magnitude of prediction errors and the computation time in estimation. For this purpose, the sensitivity of the initial values to the impact points is briefly investigated.

The following simplified equation is used for the sensitivity analysis:

$$\dot{\underline{X}}(t) = \underline{B} = \begin{bmatrix} 0 \\ 0 \\ 0 \\ 0 \\ a \\ b \end{bmatrix},$$

where a and b are constant. Then the solution is described as

$$\underline{X}(t) = \begin{bmatrix} 1 & 0 & 0 & t & 0 & 0 \\ 0 & 1 & 0 & 0 & t & 0 \\ 0 & 0 & 1 & 0 & 0 & t \\ 0 & 0 & 0 & 1 & 0 & 0 \\ 0 & 0 & 0 & 0 & 1 & 0 \\ 0 & 0 & 0 & 0 & 0 & 1 \end{bmatrix} \underline{X}(0) + \begin{bmatrix} 0 \\ \frac{1}{2} at^2 \\ \frac{1}{2} bt^2 \\ 0 \\ at \\ bt \end{bmatrix} \quad (8)$$

If there is a small error $\Delta \underline{X}$ in $\underline{X}(0)$, then the state value $\tilde{\underline{X}}(T)$ at time T is expressed as

$$\begin{aligned}
\tilde{\underline{X}}(T) &= \begin{bmatrix} 1 & 0 & 0 & T & 0 & 0 \\ 0 & 1 & 0 & 0 & T & 0 \\ 0 & 0 & 1 & 0 & 0 & T \\ 0 & 0 & 0 & 1 & 0 & 0 \\ 0 & 0 & 0 & 0 & 1 & 0 \\ 0 & 0 & 0 & 0 & 0 & 1 \end{bmatrix} [\underline{X}(0) + \underline{\Delta X}] + \begin{bmatrix} 0 \\ \frac{1}{2} aT^2 \\ \frac{1}{2} bT^2 \\ 0 \\ aT \\ bT \end{bmatrix} \\
&= \underline{X}(T) + \begin{bmatrix} 1 & 0 & 0 & T & 0 & 0 \\ 0 & 1 & 0 & 0 & T & 0 \\ 0 & 0 & 1 & 0 & 0 & T \\ 0 & 0 & 0 & 1 & 0 & 0 \\ 0 & 0 & 0 & 0 & 1 & 0 \\ 0 & 0 & 0 & 0 & 0 & 1 \end{bmatrix} \underline{\Delta X} \quad (9)
\end{aligned}$$

The examples considered previously are used again for the sensitivity analysis. In both endoatmosphere and exoatmosphere cases, 10 percent and 20 percent errors are independently introduced into each initial value. The propagation of each error to the final values is evaluated by integrating the differential Eq. (1) numerically and by using the relationship in Eq. (8). These results are shown in Tables VI through IX. The values in parentheses in these tables are theoretical results by using the relationship in Eq. (8). According to Ref. 2, the estimation errors will become about 2 percent after 5-sec of filtering. Hence, this sensitivity analysis will give better results for more realistic cases.

This coarse sensitivity analysis gives a good indication of the propagation of errors in the initial values. In the example of exoatmosphere, the sensitivity analysis and the numerical integration agree very well. In the case of endoatmosphere, the analysis and the numerical integration match very well in most cases, but the cases where errors exist in $z(0)$ and $\dot{z}(0)$ do have significant deviations. Errors in $x(0)$, $y(0)$, $\dot{x}(0)$, and $\dot{y}(0)$ propagate in the manner expressed in Eq. (9). The position errors propagate without any amplification and have little influence on the velocity. The velocity errors propagate without any amplification on the velocity itself, but they have a significant effect on the position errors.

Table VI
SENSITIVITY OF IMPACT POINTS TO INITIAL VALUES (ENVOI ATMOSPHERE), 10% Error

	\dot{x} (ft)	\dot{y} (ft)	\dot{z} (ft)	\dot{x} (ft/sec)	\dot{y} (ft/sec)	\dot{z} (ft/sec)	\ddot{x} (ft/sec ²)	\ddot{y} (ft/sec ²)	\ddot{z} (ft/sec ²)	TIME (sec)
Initial conditions	9.20640×10^3	4.51515×10^3	3.27897×10^5	-1.81864×10^4	-1.12315×10^4	-7.01397×10^3				0
Without error	1.71115×10^5	-8.67156×10^3	1.16470×10^4	-1.31774×10^4	-8.29922×10^3	-6.28133×10^3				42
10% error in $\dot{x}(0)$	2.66168×10^5	-6.82460×10^3	1.16401×10^4	-1.34881×10^4	-8.30420×10^3	-6.28115×10^3				42
9.20640 × 10 ³	(2.00479×10^5)									
10% error in $\dot{y}(0)$	1.71221×10^5	3.62746×10^4	1.16322×10^4	-1.34831×10^4	-8.30598×10^3	-6.28114×10^3				42
1.51515 × 10 ³		(3.64794×10^4)								
10% error in $\dot{z}(0)$	1.62231×10^5	-1.62075×10^4	3.90962×10^4	-1.64810×10^4	-1.01503×10^4	-7.65033×10^3				42
3.27897 × 10 ⁵			(4.44370×10^4)							
10% error in $\ddot{x}(0)$	1.69763×10^5	-8.12425×10^3	1.18714×10^4	-1.45965×10^4	-8.17112×10^3	-6.19242×10^3				42
-1.81864 × 10 ⁴	(6.98032×10^5)			(-1.32960×10^4)						
10% error in $\ddot{y}(0)$	1.77532×10^5	-5.46276×10^4	1.17902×10^4	-1.34110×10^4	-9.98473×10^3	-6.66434×10^3				42
-1.12315 × 10 ⁴		(-5.58439×10^4)			(-1.01179×10^3)					
10% error in $\ddot{z}(0)$	1.64080×10^5	1.50169×10^4	3.62683×10^4	-1.61417×10^4	-9.93909×10^3	-6.87443×10^3				42
7.01397 × 10 ³			(4.11057×10^4)			(-5.57993×10^3)				

Table VII
SENSITIVITY OF IMPACT POINTS TO INITIAL VALUES (ENDOATMOSPHERE), 20% Error

	\dot{x} (ft)	\dot{y} (ft)	\dot{z} (ft)	\ddot{x} (ft/sec)	\ddot{y} (ft/sec)	\ddot{z} (ft/sec)	TIME (sec)
Initial conditions Without error	9.20640×10^5	4.51515×10^5	3.27897×10^5	-1.81864×10^4	-1.12315×10^4	-7.01397×10^3	0
Without error	1.74115×10^5	-8.67156×10^3	1.16470×10^4	-1.31774×10^4	-8.29922×10^3	-6.28133×10^3	42
20% error in $\dot{x}(0)$ 1.81128×10^5	3.58111×10^5 (3.58515×10^5)	-8.82345×10^3	1.16516×10^4	-1.34934×10^4	-8.30476×10^3	-6.28116×10^3	42
20% error in $\dot{y}(0)$ 9.63030×10^4	1.74220×10^5	8.13691×10^4 (8.16304×10^4)	1.16348×10^4	-1.34832×10^4	-8.30824×10^3	-6.28112×10^3	42
20% error in $\dot{z}(0)$ 6.55764×10^4	1.58225×10^5	-1.86765×10^4	7.01028×10^4 (7.72270×10^4)	-1.76660×10^4	-1.08801×10^4	-8.18900×10^3	42
20% error in $\ddot{x}(0)$ -3.63738×10^3	2.75209×10^4 (2.16449×10^4)	-7.42040×10^3	1.21200×10^4	-1.56703×10^4 (-1.71147×10^4)	-8.03981×10^3	-6.10436×10^3	42
20% error in $\ddot{y}(0)$ -2.24630×10^3	1.74864×10^5	-1.00375×10^5 (-1.03016×10^5)	1.19600×10^4	-1.33354×10^4	-9.85397×10^3 (-8.52385×10^3)	-6.21215×10^3	42
20% error in $\ddot{z}(0)$ 1.46279×10^3	1.59562×10^5	-1.77486×10^4	6.37924×10^4 (7.05642×10^4)	-1.74082×10^4	-1.07166×10^4	-6.73151×10^3 (-6.14105×10^3)	42

Table VIII
SENSITIVITY OF IMPACT POINTS TO INITIAL VALUES (EXOATMOSPHERE), 10% Error

	\bar{x} (ft)	\bar{y} (ft)	\bar{z} (ft)	$\dot{\bar{x}}$ (ft/sec)	$\dot{\bar{y}}$ (ft/sec)	$\dot{\bar{z}}$ (ft/sec)	TIME (sec)
Initial conditions Without error	5.19734×10^6	3.12073×10^6	1.10172×10^6	-1.72242×10^4	-1.08899×10^4	3.58640×10^2	0
Without error	9.20725×10^5	4.52091×10^5	3.26270×10^5	-1.61813×10^4	-1.12262×10^4	-7.03105×10^3	240
10% error in $x(0)$ 5.19734×10^5	1.42377×10^6 (1.44027×10^6)	4.52638×10^5	3.37995×10^5	-1.83348×10^4	-1.12245×10^4	-6.94433×10^3	240
10% error in $y(0)$ 3.12073×10^5	9.21297×10^5	7.52810×10^5 (7.64161×10^5)	3.31851×10^5	-1.81832×10^4	-1.13253×10^4	-6.98812×10^3	240
10% error in $z(0)$ 1.10172×10^5	9.22606×10^5	4.52654×10^5	4.46100×10^5 (4.36440×10^5)	-1.81738×10^4	-1.12241×10^4	-6.94570×10^3	240
10% error in $\dot{x}(0)$ -1.72242×10^3	5.12279×10^5 (5.07144×10^5)	4.53779×10^5	3.19512×10^5	-1.98422×10^4 (-1.99037×10^4)	-1.12124×10^4	-7.08991×10^3	240
10% error in $\dot{y}(0)$ -1.08899×10^3	9.19101×10^5	1.93356×10^5 (1.90733×10^5)	3.27596×10^5	-1.81693×10^4	-1.22787×10^4 (-1.23152×10^4)	-7.02033×10^3	240
10% error in $\dot{z}(0)$ 3.58640×10^2	9.20651×10^5	4.51554×10^5	3.37167×10^5 (4.12344×10^5)	-1.81868×10^4	-1.12313×10^4	-6.97452×10^3 (-6.67241×10^3)	240

Table IX

SENSITIVITY OF IMPACT POINTS OF INITIAL VALUES (EXOSPHERE), 20% Error

	x (ft)	y (ft)	z (ft)	\dot{x} (ft/sec)	\dot{y} (ft/sec)	\dot{z} (ft/sec)	\ddot{x} (ft/sec ²)	\ddot{y} (ft/sec ²)	\ddot{z} (ft/sec ²)	TIME (sec)
Initial conditions Without error	5.14739×10^6	3.12073×10^6	1.10172×10^6	-1.72242×10^4	-1.08899×10^4	3.58640×10^2	0			0
Without error	9.20525×10^5	4.52091×10^5	3.26270×10^5	-1.81613×10^4	-1.12262×10^4	-7.03105×10^3	240			240
20% error in $x(0)$ 1.03938×10^6	1.92737×10^6 (1.99910×10^6)	4.53844×10^5	3.48666×10^5	-1.84786×10^4	-1.12166×10^4	-6.86585×10^3	240			240
20% error in $y(0)$ 6.23136×10^5	9.21917×10^5	1.05424×10^6 (1.07623×10^6)	3.35778×10^5	-1.81800×10^4	-1.14181×10^4	-6.95929×10^3	240			240
20% error in $z(0)$ 2.20314×10^5	9.24328×10^5	4.51759×10^5	5.63739×10^5 (5.46614×10^5)	-1.81615×10^4	-1.12165×10^4	-6.87916×10^3	240			240
20% error in $\dot{x}(0)$ 3.41881×10^3	1.03860×10^5 (0.93763×10^5)	4.56039×10^5	3.10807×10^5	-2.14971×10^4 (-2.16261×10^4)	-1.11930×10^4	-7.16408×10^3	240			240
20% error in $\dot{y}(0)$ -2.17768×10^3	9.17461×10^5	-6.34050×10^4 (-7.00240×10^4)	3.26896×10^5	-1.82126×10^4	-1.33259×10^4 (-1.34042×10^4)	-7.02660×10^3	240			240
20% error in $\dot{z}(0)$ 7.17286×10^2	9.20551×10^5	4.51579×10^5	3.45980×10^5 (4.98417×10^5)	-1.81877×10^4	-1.12311×10^4	-6.93596×10^3 (-6.31377×10^3)	240			240

VI CONCLUSION

The differential Eq. (1) is a good mathematical model of the ballistic motion. Without any approximation, it seems hopeless to find a closed-form solution of Eq. (1). The only way to find a solution of Eq. (1) is numerical integration. As a result, it requires a significant amount of computation time. This memorandum describes a simplification of the differential Eq. (1) of the ballistic trajectories. The main purpose of an approximation is to obtain a closed-form solution.

The problems are divided into two domains, namely the endoatmospheric problem and the exoatmospheric problem. The endoatmospheric problem is again divided into two: namely, the high- β case and the low- β case. In each case, the influences of the eccentricity e , the rotation rate ω , the ballistic coefficient β , and the nonlinearities are considered. A summary of the influences is shown in Table X. In exoatmospheric prediction problems, the earth rotation rate ω and the nonlinear term \underline{C} should be treated carefully, and in endoatmospheric prediction problem, the ballistic coefficient β should be handled properly. The effect of the ballistic coefficient is very significant on the trajectory at low altitudes (e.g., for impact point and impact time prediction). Further research effort should be oriented toward improving the estimation and prediction of ballistic coefficients.

Future work on the prediction problem is to obtain closed-form solutions of Eqs. (3) and (7). One possible way is to find a piecewise closed-form solution over a suitable time interval by taking constant values of β , \underline{C} and \tilde{C} in Eqs. (3) and (7), respectively.

Table X
SUMMARY OF INFLUENCES OF e , ω , \underline{C} , AND β

		e	ω	\underline{C}	SENSITIVITY OF β
		negligible	significant	significant	β is negligible sensitivity is zero
Endo- Atmosphere	High β	negligible	negligible	negligible	low sensitivity
	Low β	negligible	negligible	significant	high sensitivity

APPENDIX

The derivation of the differential Eq. (1) is discussed in this appendix.

If ${}^N \underline{a}^P$ is the absolute acceleration of a missile P (it is considered to be a particle) in a reference frame N and m is the mass of P , then the inertia force \underline{F} acting on P in N satisfies

$$\underline{F} = m {}^N \underline{a}^P \quad (\text{A.1})$$

The reference frame N is a reference frame in which the center C of the earth and the earth's axis, line NS , are fixed such that the angular velocity of the earth E with respect to the reference N , ${}^N \underline{\omega}^E$, is given by

$${}^N \underline{\omega}^E = \underline{\omega} = \omega \hat{n}$$

where $\omega = 2\pi$ rad/day and \hat{n} is a unit vector parallel to line NS . This reference frame N is a good approximation to a Newtonian reference frame. From Fig. 1,

$$\underline{E} = x \hat{i} + y \hat{j} + z \hat{k}$$

where \hat{i} , \hat{j} and \hat{k} are unit vectors defined in Fig. 1 and x , y , and z are the measure numbers in the directions \hat{i} , \hat{j} , and \hat{k} , respectively. The velocity of P with respect to the reference E is then expressed⁵ as

$$\underline{v}^P = \frac{d\underline{E}}{dt} = \dot{x} \hat{i} + \dot{y} \hat{j} + \dot{z} \hat{k}$$

The accelerations ${}^E \underline{a}^P$, ${}^N \underline{a}^P$ at time t^* are related by

$${}^N \underline{a}^P = {}^E \underline{a}^P + {}^N \underline{a}^{P^*} + 2\underline{\omega} \times \underline{v}^P \quad (\text{A.2})$$

⁵ $\frac{d}{dt}$ reads the time derivative (*) with respect to E .

where P^* is the point fixed in E that coincides with P at time t^* , and $N_{\underline{a}^{P^*}}$ is called the coincident-point velocity and the vector $2\omega \times \underline{E}V^P$ is called the coriolis acceleration of P for the reference frames E and N .

The coincident point velocity $N_{\underline{a}^{P^*}}$ satisfies

$$N_{\underline{a}^{P^*}} = N_{\underline{a}^C} N_{\underline{a}^E} \times \underline{r} + \underline{\omega} \times (\underline{\omega} \times \underline{r})$$

and

$$N_{\underline{a}^C} = 0, \quad N_{\underline{a}^E} = \frac{N d\omega}{dt} = 0$$

The acceleration of P with respect to E is

$$\underline{E} \underline{a}^P = \frac{E d \underline{E} V^P}{dt} = \dot{\hat{x}} \hat{i} + \dot{\hat{y}} \hat{j} + \dot{\hat{z}} \hat{k}$$

Therefore,

$$N_{\underline{a}^P} = \dot{\hat{x}} \hat{i} + \dot{\hat{y}} \hat{j} + \dot{\hat{z}} \hat{k} + \underline{\omega} \times (\underline{\omega} \times \underline{r}) + 2\underline{\omega} \times \underline{E}V^P \quad (A.3)$$

Since $\underline{\omega}$ and \underline{r} are expressed as

$$\begin{aligned} \underline{\omega} &= \omega \sin \mu \hat{k} + \omega \cos \mu \hat{j} \\ \underline{r} &= r_x \hat{i} + r_y \hat{j} + r_z \hat{k} \\ r_x &= x \\ r_y &= y - R \sin(\mu - \mu_c) \\ r_z &= z + R \cos(\mu - \mu_c) \end{aligned} \quad (A.4)$$

The last two terms of Eq. (A.3) are written as

$$\begin{aligned} \underline{\omega} \times (\underline{\omega} \times \underline{r}) &= \underline{\omega} \cdot \underline{r} \underline{\omega} \\ &= -\omega^2 r_x \hat{i} + \omega^2 [(r_y \cos \mu + r_z \sin \mu) \cos \mu - r_y] \hat{j} \\ &\quad + \omega^2 [(r_y \cos \mu + r_z \sin \mu) \sin \mu - r_z] \hat{k} \\ \underline{\omega} \times \underline{E}V^P &= \omega(\dot{z} \cos \mu - \dot{y} \sin \mu) \hat{i} + \dot{x} \omega \sin \mu \hat{j} - \dot{x} \omega \cos \mu \hat{k} \end{aligned}$$

Therefore,

$$\begin{aligned} \underline{N}_{d^P} = & \{\dot{x} + 2\omega(\dot{z} \cos \mu - \dot{y} \sin \mu)\} \hat{i} \\ & + \{\dot{y} + 2\dot{x}\omega \sin \mu + \omega^2(r_y \cos \mu + r_z \sin \mu) \cos \mu\} \hat{j} \\ & + \{\dot{z} - 2\dot{x}\omega \cos \mu + \omega^2(r_y \cos \mu + r_z \sin \mu) \sin \mu\} \hat{k} \end{aligned} \quad (\text{A.5})$$

Let us now consider the left-hand side of Eq. (A.1). The force \underline{F} acting on a missile P is divided into two elements, namely the drag force \underline{F}_d and the gravitational force \underline{F}_g ; hence,

$$\underline{F} = \underline{F}_d + \underline{F}_g \quad (\text{A.6})$$

The drag force per unit mass acting on a body is given approximately by the equation

$$\underline{F}_d = - \frac{m\mathcal{L}}{2\beta} |\underline{V}^P| \underline{V}^P \quad (\text{A.7})$$

Next, let us find the expression of the gravitational force.

The gravitational potential at P due to the earth E is expressed⁶ as

$$U^{E/P} = \frac{G}{r} \left\{ m - \frac{1}{2r^2} [3I - (I_l + I_n + I_n)] \right\} + \dots$$

where I is the moment of inertia about the line OP and I_l , I_n , and I_n are the principal moments of inertia of the earth E of the mass m .

Since the gravitational force per unit mass is the gradient of the gravitational potential, the equation

$$\underline{F}_g/m = \nabla U^{E/P}$$

holds, where the operator ∇ is defined as

$$\nabla = \hat{l} \frac{\partial}{\partial X_1} + \hat{m} \frac{\partial}{\partial X_2} + \hat{n} \frac{\partial}{\partial X_3}$$

and X_1 , X_2 and X_3 are measure numbers of the principal axes of the earth E . Let us define mutually perpendicular unit vectors \hat{k}_1 and \hat{k}_2 as shown in Fig. A-1. Then

$$\begin{aligned} \underline{F}_g/m &= \nabla U^{E/P} \\ &= \frac{GM}{r^2} \hat{k}_1 + \frac{3G}{2r^4} [(-2I_1 + I_2 + I_3)\hat{k}_1 \\ &\quad + 2I_{12}\hat{k}_2 + 2I_{13}\hat{k}_3] \end{aligned}$$

where I_1 , I_2 , I_3 are the moments of inertia of the earth about the center along the directions \hat{n}_1 , \hat{n}_2 , \hat{n}_3 , respectively, and I_{12} , I_{13} are the moment of inertia of the earth about the center for the pair of directions \hat{n}_1 , \hat{n}_2 and \hat{n}_1 , \hat{n}_3 respectively.

By using algebraic transformation, the above equation becomes

$$\begin{aligned} \underline{F}_g/m &= \nabla U^{E/P} = \frac{GM}{r^2} \hat{k}_1 + \frac{3G}{r^4} (I_n - I_a)(1 - 5 \sin^2 \phi) \hat{k}_1 \\ &\quad - \frac{3G}{2r^4} (I_n - I_a) 2 \sin \phi \hat{n} \end{aligned}$$

If

$$J = \frac{3(I_n - I_a)}{2Ma^2}$$

and

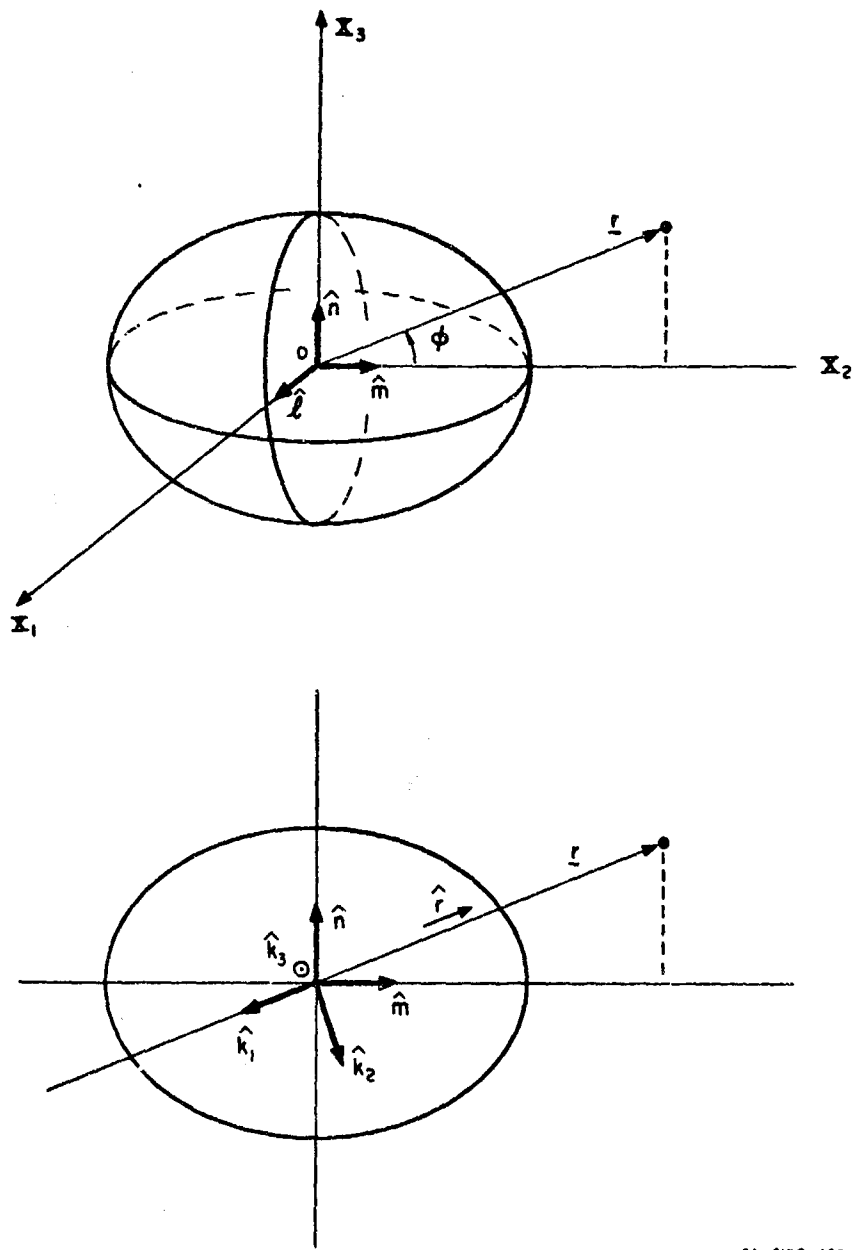
$$\hat{r} = -\hat{k}_1$$

then

$$\underline{F}_g/m = g_r \hat{r} + g_n \hat{n} \quad , \quad (A.8)$$

where

$$\begin{aligned} g_r &= -\frac{GM}{r^2} \left[1 + J \left(\frac{a}{r} \right)^2 (1 - 5 \sin^2 \phi) \right] \\ g_n &= -\frac{2GM}{r^2} J \left(\frac{a}{r} \right)^2 \sin \phi \end{aligned}$$



TA-5188-480

FIG. A-1 ILLUSTRATIONS OF UNIT VECTORS

Unit vectors \hat{r} and \hat{n} are described in terms of \hat{i} , \hat{j} , and \hat{k} as follows:

$$\hat{r} = \frac{r_x}{|r|} \hat{i} + \frac{r_y}{|r|} \hat{j} + \frac{r_z}{|r|} \hat{k}, \quad |r| = \sqrt{r_x^2 + r_y^2 + r_z^2}$$

$$\hat{n} = \cos \mu \hat{j} + \sin \mu \hat{k}.$$

Hence Eq. (A.7) is expressed as

$$\underline{E}_g/m = g_r \frac{r_x}{|r|} \hat{i} + \left(g_r \frac{r_y}{|r|} + g_n \cos \mu \right) \hat{j} + \left(g_r \frac{r_z}{|r|} + g_n \sin \mu \right) \hat{k}. \quad (\text{A.9})$$

By substituting Eqs. (A.5), (A.7) and (A.9) into Eq. (A.1) and comparing the measure values of \hat{i} , \hat{j} , \hat{k} elements, it is found that

$$\left. \begin{aligned} \ddot{x} + 2\omega(\dot{z} \cos \mu - \dot{y} \sin \mu) - \omega^2 r_x &= -\frac{\rho}{2\beta} V \dot{x} + g_r \frac{r_x}{|r|} \\ \ddot{y} + 2\omega \dot{x} \sin \mu - \omega^2 r_y \sin^2 \mu \\ &+ \omega^2 r_z \sin \mu \cos \mu = -\frac{\rho}{2\beta} V \dot{y} + g_r \frac{r_y}{|r|} + g_n \cos \mu \\ \ddot{z} - 2\omega \dot{x} \cos \mu - \omega^2 r_z \cos^2 \mu \\ &+ \omega^2 r_y \sin \mu \cos \mu = -\frac{\rho}{2\beta} V \dot{z} + g_r \frac{r_z}{|r|} + g_n \sin \mu \end{aligned} \right\} \quad (\text{A.10})$$

where

$$\begin{aligned} r_x &= x \\ r_y &= y - R \sin(\mu - \mu_c) \\ r_z &= z + R \cos(\mu - \mu_c) \\ r &= (r_x^2 + r_y^2 + r_z^2)^{1/2} \\ V &= (\dot{x}^2 + \dot{y}^2 + \dot{z}^2)^{1/2} \\ g_r &= -\frac{GM}{r^2} \left\{ 1 + J \left(\frac{a}{r} \right)^2 (1 - 5 \sin^2 \phi) \right\} \end{aligned}$$

$$g_n = - \frac{2GM}{r^2} J \left(\frac{a}{r} \right)^2 \sin \phi$$

$$\sin \phi = \frac{1}{r} \left\{ y \cos \mu + z \sin \mu + R \sin \mu_c \right\} .$$

If a 6×1 vector \underline{X} is defined as

$$\underline{X}^T = [x, y, z, \dot{x}, \dot{y}, \dot{z}] ,$$

then Eq. (A.10) is written as Eq. (1) in the main text.

REFERENCES

1. R. E. Kalman, "A New Approach to Linear Filtering and Prediction Problems," *Trans. ASME, J. Basic Engr.* (March 1960).
2. R. E. Larson, R. M. Dressler, R. S. Patner, "Application of the Extended Kalman Filter to Ballistic Trajectory Estimation," Final Report, Contract DA-01-021-AMC-90006(Y), SRI Project 5188-103, Stanford Research Institute, Menlo Park, California (January 1967).
3. U.S. Standard Atmosphere, 1962, Prepared by NASA, USAF, USWB (December 1962).
4. Nike-Zeus TIC Equations, Bell Telephone Laboratories.
5. T. R. Kane, *Analytical Elements of Mechanics*, Vol. 2 (Academic Press, 1961).
6. S. W. McCuskey, *Introduction to Celestial Mechanics* (Addison-Wesley, 1963).